

## REVIEW

[View Article Online](#)  
[View Journal](#) | [View Issue](#)Cite this: *J. Mater. Chem. A*, 2024, 12, 28682

## Advances in radiative cooling materials for building energy efficiency: a decade of progress

Ke Huang,<sup>id</sup><sup>a</sup> Zhixin Huang,<sup>a</sup> Yahui Du,<sup>\*a</sup> Yan Liang,<sup>bc</sup> Junwei Liu<sup>id</sup><sup>\*bc</sup> and Jinyue Yan<sup>\*bc</sup>

Cooling systems are responsible for consuming 15% of global electricity and contributing to 10% of global carbon emissions. The emerging radiative sky cooling (RSC) technology provides an efficient means to dissipate building heat through the atmospheric window and reduce reliance on evaporation–compression cooling systems. Extensive global efforts have demonstrated the significant energy-saving potential of RSC technology in buildings. In this critical review, we present a comprehensive analysis of the advancements made in RSC technology over the past decade, a fast-developing period, to further facilitate its practical applications in buildings. Firstly, we discuss the detailed design requirements of building-integrated RSC materials, emphasizing the need for large-scale implementation, cost-effectiveness, multiple color options, durability, bifunction and self-adaption. Subsequently, we systematically examine the cooling performance and the existing challenges associated with various RSC materials to clarify their applications in buildings. Furthermore, we delve into the discussions on the utilization of RSC materials in buildings, focusing on three main areas: direct building cooling, building cooling devices, and systems. Finally, we address the remaining challenges and provide our insights to propel the advancement of practical applications of RSC technology.

Received 17th July 2024  
Accepted 23rd September 2024

DOI: 10.1039/d4ta04942j

[rsc.li/materials-a](https://rsc.li/materials-a)

## 1 Introduction

Buildings account for approximately 30% of global final energy consumption and contribute to around 26% of global carbon emissions, exacerbating energy crisis and global warming.<sup>1</sup> The energy demand in buildings has been experienced in an annual growth rate of over 1%, which is projected to further rise due to the significant increase in global floor area by approximately 15% by 2030. In a net-zero emission scenario, it is expected that building energy consumption should be dropped by ~25% and fossil fuel should be decreased by over 40% in 2030.<sup>1</sup> To fulfill this target, worldwide efforts have been devoted to building energy efficiency, especially for cooling systems of buildings. Cooling has emerged as a primary driver of electricity demand in buildings, with an estimated 2 billion air-conditioning devices in operation worldwide. This widespread use of air-conditioning systems highlights the significant impact of cooling on energy consumption within built environments.<sup>2</sup>

Generally, the operation of cooling systems accounts for 15% of global electricity and results in 10% of global carbon

emissions.<sup>3</sup> Since 1990, the energy consumption for building cooling has more than tripled and the value in 2022 was further increased by over 5% from 2021.<sup>4</sup> In hot countries and regions, the electricity demand for building cooling with air-conditioning devices is increased by over 50% in summer and cooling accounts for over 70% of electricity peak demand.<sup>4</sup> Besides significant energy consumption, the existing air-conditioning devices also result in a series of issues, *e.g.*, global warming potential, ozone depletion, water resource consumption and annoying noise.<sup>5</sup> Accordingly, developing novel cooling methods may be the promising routes to address these challenges and reduce cooling energy consumption. Thermoelectric coolers have been employed in some compact devices, but the high power consumption places great restrictions on the actual applications in buildings.<sup>6–8</sup> Some emerging cooling methods (*e.g.*, magnetocaloric cooling, electrocaloric cooling and elastocaloric cooling) are only in the laboratory stage and far away from large-scale applications.<sup>9–12</sup>

In contrast, radiative sky cooling (RSC) technology has witnessed great advance over the past decade (Fig. 1).<sup>33–37</sup> and has already been attempted to provide cooling for buildings.<sup>3,38,39</sup> Generally, RSC technology is mainly dependent on the atmospheric window of 8–13  $\mu\text{m}$ , which can dissipate heat into the outer space with a temperature of ~3 K.<sup>40–42</sup> The early radiative coolers generally employed complicated and costly photonic structures, which are not favorable for the actual applications of this technology.<sup>26,27,43</sup> In 2013, Fan's group proposed a 2D

<sup>a</sup>School of Environmental Science and Engineering, State Key Laboratory of Engines, Tianjin University, Tianjin, 300350, China. E-mail: duyahui0608@tju.edu.cn<sup>b</sup>International Centre of Urban Energy Nexus, The Hong Kong Polytechnic University, Kowloon, Hong Kong<sup>c</sup>Department of Building Environment and Energy Engineering, The Hong Kong Polytechnic University, Kowloon, Hong Kong. E-mail: junweiliu@polyu.edu.hk; jinyan@polyu.edu.hk

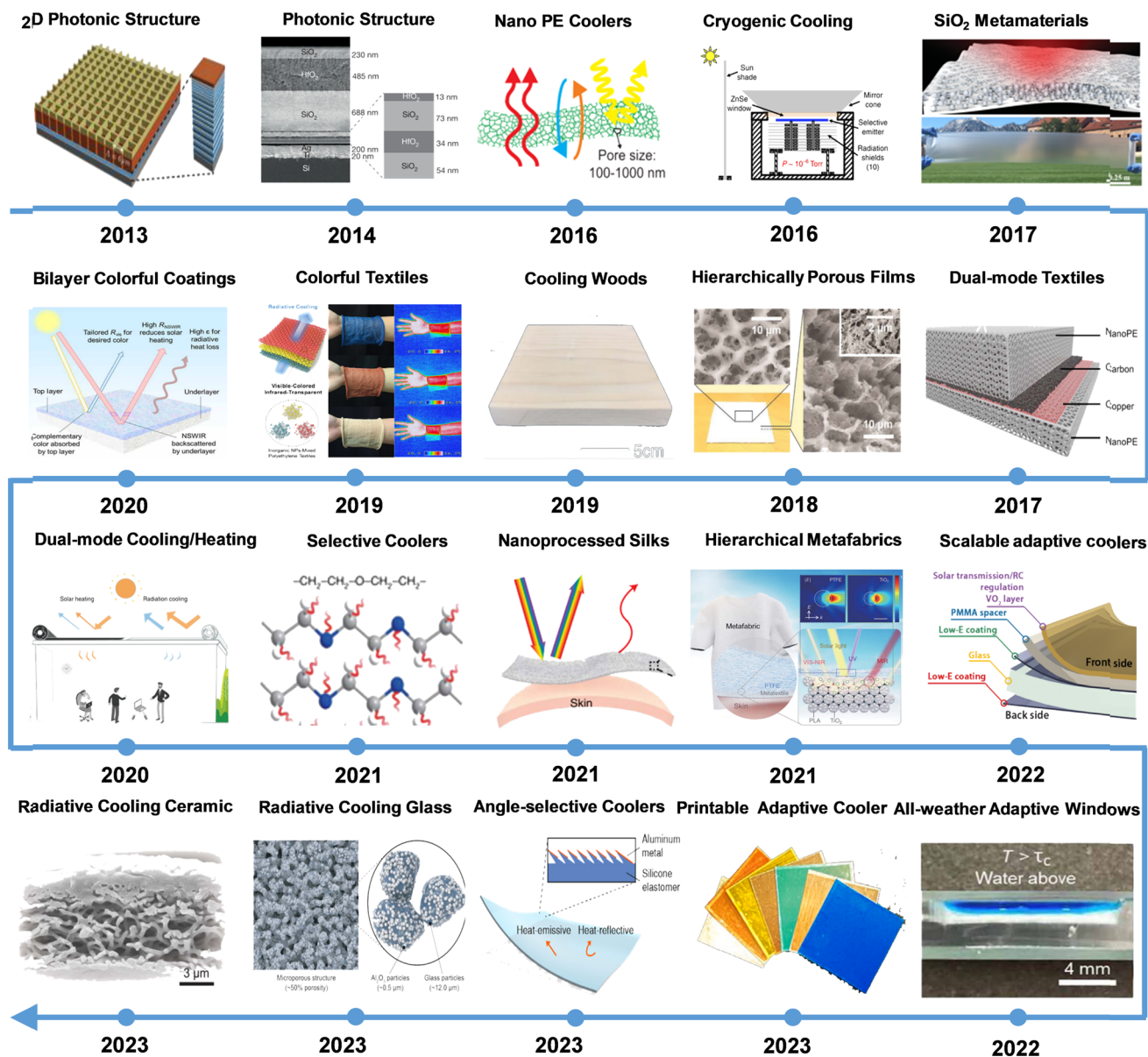


Fig. 1 The progress of radiative cooling materials and their applications over the past decade. Reproduced with permission from ref. 13–23 Copyright 2016–2023 AAAS. Ref. 24–28 Copyright 2014, 2016, 2020 and 2021 Springer Nature. Ref. 29 Copyright 2013, American Chemical Society. Ref. 30–32 Copyright 2019 and 2023, Elsevier.

photonic structure to achieve daytime cooling performance.<sup>29</sup> Subsequently, the group developed the promising multilayer photonic structure for daytime cooling performance with a sub-ambient temperature of 4.9 K.<sup>27</sup> Furthermore, promising large-scale RSC materials (glass–polymer hybrid metamaterials<sup>23</sup> and hierarchically porous polymer coatings<sup>22</sup>) were developed and can be facilely integrated with buildings and air-conditioning systems.<sup>38,39,44</sup> Moreover, RSC building materials were developed *via* the complete delignification and densification of ordinary woods, which can significantly enhance solar back-scattering and infrared emission, resulting in a great energy saving of 20–40% in the United States.<sup>21</sup>

On the other hand, there are also abundant application attempts of RSC technology in building cooling. In 2017, Fan's

group developed the first daytime cooling panels with cool fluids below the ambient temperature *via* RSC technology.<sup>3</sup> The developed panels could provide a cooling temperature drop of 5 °C and cooling power of 70 W m<sup>-2</sup>, which could enable a great electricity saving potential of 21% for a two-storey office building in Las Vegas. In addition, Zhao *et al.* designed radiative cooling modules based on low-cost cooling metamaterials, which can cool water by ~10.6 °C below the ambient temperature at noon.<sup>38</sup> Kilowatt-scale cooling systems (13.5 m<sup>2</sup> cooling area) were further developed and could provide a maximum cooling power of 1296 W for buildings. Further modeling results revealed that the cooling modules could enable a building electricity saving of 32–45% in three different locations of the United States.<sup>39</sup>

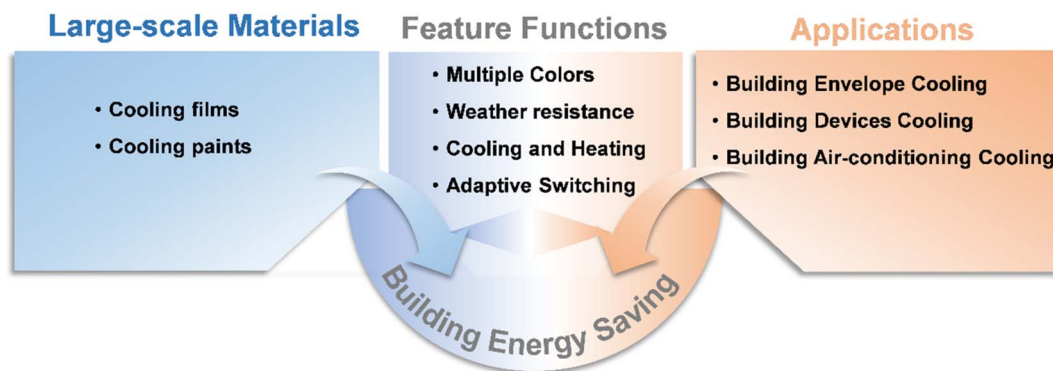


Fig. 2 The scope and structure of this review paper covering materials to applications for building energy saving.

The early cooling materials and application attempts reveal the great energy saving potential of RSC technology in buildings. However, the practical implementation of this technology in buildings necessitates specific requirements for cooling materials and devices. Within the past decade, the technology has witnessed great advance in developing cooling materials and devices for building applications.<sup>45–47</sup> It is highly desirable to contribute a timely review of past-decade efforts for the commercial applications of RSC technology.

Herein, we contribute a comprehensive review of the past decade's research efforts in advancing the actual applications of RSC technology in buildings (Fig. 2). The principles of radiative cooling for efficient building cooling are firstly introduced for guiding the material design. Subsequently, the detailed requirements of RSC materials are discussed for building applications, mainly including scalability, low cost, multiple colors, durability, dual function and self-adaption. Afterwards, the design and cooling performance of various cooling materials are systematically discussed to highlight their great benefits in countering external thermal disturbance and fulfilling multiple functions in buildings. Moreover, the applications of RSC materials in buildings are further summarized from three perspectives, including building envelope cooling, building device cooling and building air-conditioning cooling. Finally, the remaining challenges and our insights are delivered for the actual applications of RSC technology.

## 2 Fundamentals of radiative cooling in buildings

The application of radiative cooling materials to buildings has been widely explored.<sup>48,49</sup> In general, the radiative cooling power can be calculated as follows.

$$P_{\text{cool}}(T_r) = P_r(T_r) - P_a(T_a) - P_{\text{solar}} - P_{\text{cond+conv}} \quad (1)$$

$P_r(T_r)$  is the power dissipated by the radiative coolers of area  $A$  and can be expressed as<sup>50</sup>

$$P_r(T_r) = 2\pi A \int_0^{\pi/2} d\theta \sin \theta \cos \theta \int_0^{\infty} d\lambda I_B(T_r, \lambda) \varepsilon(\lambda, \theta) \quad (2)$$

$P_a(T_a)$  is the atmospheric emissive power absorbed by the radiative coolers and can be expressed as<sup>35</sup>

$$P_a(T_a) = 2\pi A \int_0^{\pi/2} d\theta \sin \theta \cos \theta \int_0^{\infty} d\lambda I_B(T_a, \lambda) \varepsilon(\lambda, \theta) \varepsilon_a(\lambda, \theta) \quad (3)$$

where  $I_B(T, \lambda)$  is the spectral radiation of a black body with the radiative temperature of  $T_r$  or ambient temperature  $T_a$  at any wavelength  $\lambda$  by Plank's law.

$\varepsilon_a(\lambda, \theta)$  is the spectral and angular emissivity of the atmosphere and can be defined as<sup>51</sup>

$$\varepsilon_a(\lambda, \theta) = 1 - t(\lambda)^{1/\cos(\theta)} \quad (4)$$

where  $t(\lambda)$  is the atmospheric transmissivity in the zenith direction.

$P_{\text{solar}}$  is the solar radiation absorbed by the radiative coolers and can be given by<sup>52</sup>

$$P_{\text{solar}} = A \int_0^{\infty} d\lambda \varepsilon_s(\lambda, 0) I_{\text{solar}}(\lambda) \quad (5)$$

where  $I_{\text{solar}}(\lambda)$  is the solar illumination and  $\varepsilon_s(\lambda, 0)$  is the solar absorptivity of the radiative coolers at a fixed angle 0.

$P_{\text{cond+conv}}(T_r, T_a)$  is the power loss due to convection and conduction (non-radiative heat exchange) and can be expressed as

$$P_{\text{cond+conv}}(T_r, T_a) = Ah_c(T_a - T_r) \quad (6)$$

where  $h_c = h_{\text{cond}} + h_{\text{conv}}$  is a combined non-radiative heat exchange stemming from the conductive and convective heat exchange between the radiative coolers and the ambient environment. The non-radiative heat exchange coefficient can be expressed as<sup>38</sup>

$$h_c = 2.5 + 2v \quad (7)$$

where  $v$  is the wind speed,  $\text{m s}^{-1}$ .

The amount of energy savings generated by radiative cooling in buildings can be calculated based on the conservation of energy.

$$P_{\text{cool}}(T_r) = -\frac{T_{\text{out}} - T_{\text{air}}}{R}$$



where  $T_{\text{out}}$  is the temperature of the building outside the façade, °C,  $T_{\text{in}}$  is the temperature inside the façade, °C, and  $R$  is the thermal resistance of the façade.

### 3 Basic requirements of radiative cooling materials in buildings

With the worldwide efforts, RSC materials have achieved great advance in cooling performance, especially for solar reflectivity, which has great impact on the cooling supply under the strong solar radiation. For actual applications, RSC materials should have two critical features: scalability and low cost. In this section, we summarize the past-decade advance of large-scale and cost-effective RSC materials in two sub-sections, namely, cooling films and paints.

#### 3.1 Cooling films

Since the breakthrough of daytime radiative cooling in 2014,<sup>27</sup> worldwide research efforts have been devoted to developing scalable RSC materials with low cost.<sup>53–55</sup> In 2015, Smith's group investigated the cooling performance of super-cool roof materials with birefringent polymer pairs, which can be mass-produced for commercial products.<sup>56</sup> The super-cool materials can achieve a high solar reflectivity of 97% and infrared emissivity of 96%, resulting in a sub-ambient temperature drop of 2 °C under strong solar radiation ( $1060 \text{ W m}^{-2}$ ). In 2017, Yang and Yin's group developed scalable glass-polymer hybrid metamaterials *via* embedded resonant dielectric microspheres in a polymeric matrix and backscattering silver layer (Fig. 3a and b), which can enable a high solar reflectivity of 96% and infrared emissivity of 93%.<sup>23</sup> The developed metamaterials can be processed *via* roll-to-roll methods with an ultra-low cost of

$\$0.25\text{--}0.5 \text{ m}^{-2}$ , which can significantly advance the commercial applications of RSC technology. Although silver coatings for solar reflection offer significant benefits, they are prone to oxidation when exposed to air. This susceptibility to oxidation can limit their practical applications. Furthermore, the use of silver materials can inadvertently contribute to light pollution, which poses another obstacle to the widespread adoption of this technology.

In contrast, porous cooling films provide a viable solution to replace the notorious silver mirrors for solar reflection. These films utilize Mie scattering to enable strong solar reflection while addressing the issue of light pollution.<sup>59–62</sup> Fan and Zhou's group developed scalable particle-embedded porous coolers *via* the promising electrospinning method, which has been widely used to process high-performance and large-scale RSC materials.<sup>55</sup> Additionally, the phase inversion method, phase separation method, and roll-to-roll method are also desirable for developing porous-based radiative cooling films.<sup>63</sup> For instance, Tian *et al.* developed a hierarchically porous film *via* a super-large-scale film-stretching roll-to-roll method.<sup>58</sup> The developed porous films presented a high solar reflectivity of 97.6% and infrared emissivity of 90.1%, which can enable an average mid-day temperature drop of 7.92 °C and cooling power of  $116.0 \text{ W m}^{-2}$  (Fig. 3c and d). Moreover, the introduction of micro-nano particles into porous cooling films can substantially enhance radiative cooling performance, and has been widely employed in RSC material design.<sup>55,62,64</sup>

Recently, some promising reports proposed that cooling materials with high thermal resistance have great application potential in buildings due to their capability of blocking thermal disturbance.<sup>65–69</sup> For instance, Zhou *et al.* developed low-cost and sustainable polydimethylsiloxane sponges with a porous structure, which can deliver a solar reflectivity of 93%

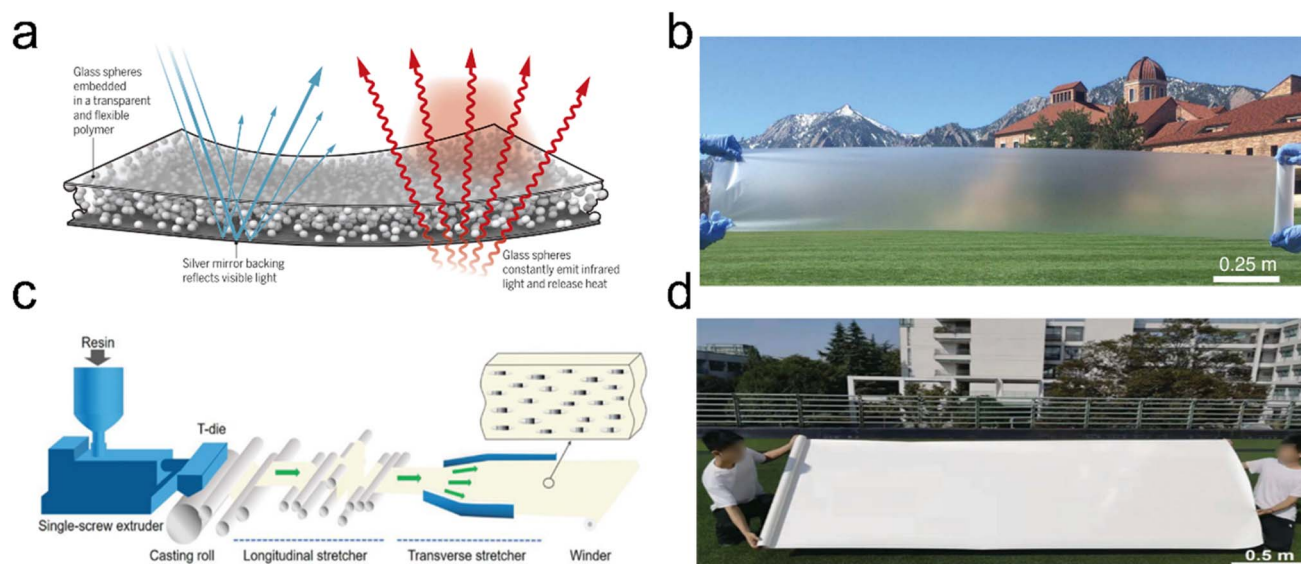


**Fig. 3** The early large-scale radiative cooling materials. (a) Schematic of glass-polymer hybrid metamaterials. (b) Photograph of large-scale glass-polymer hybrid metamaterials. (c) Schematic of the super-large-scale fabrication of hierarchically porous film. (d) Photograph of a roll of the fabricated hierarchically porous film. (a) Reproduced with permission from ref. 57 Copyright 2017 AAAS. (b) Reproduced with permission from ref. 23 Copyright 2017 AAAS. (c and d) Reproduced with permission from ref. 58 Copyright 2022 Wiley.



and infrared emissivity of 96%, resulting in a sub-ambient temperature drop of  $\sim 4.6$  °C and cooling power of  $43 \text{ W m}^{-2}$ .<sup>66</sup> Moreover, the promising sponges presented a low thermal conductivity of  $\sim 0.06 \text{ W (m}^{-1} \text{ K}^{-1})$ , which can significantly prevent external heat disturbance from entering the indoor environment and preserve the cooling capacity in buildings. Additionally, aerogel materials have been widely used in thermal insulation of buildings due to their ultra-low thermal conductivity and high-temperature resistance, which are also critical properties for developing RSC materials for buildings.<sup>65,70–73</sup> Liu *et al.* developed superhydrophobic poly(lactic acid) aerogels with a low thermal conductivity of  $0.037 \text{ W (m}^{-1} \text{ K}^{-1})$  and high compression strength of  $0.1 \text{ MPa}$ . The aerogel-based coolers could achieve a solar reflectivity of 89% and infrared emissivity of 93%, enabling a daytime temperature drop of  $\sim 3.5$  °C.<sup>69</sup> Moreover, Li *et al.* developed promising

silica–alumina nanofibrous aerogels with a higher solar reflectivity of 95% and infrared emissivity of 93%, which enable a daytime temperature drop of  $\sim 5$  °C.<sup>70</sup> The thermal conductivity of silica–alumina aerogels can be significantly reduced to  $\sim 0.03 \text{ W (m}^{-1} \text{ K}^{-1})$ , highlighting their immense potential for application in buildings. Recent reports, such as the study conducted by Cai *et al.*, have demonstrated similar findings. Their research revealed that aerogel coolers could achieve a substantial reduction in cooling energy consumption by  $\sim 35.4\%$  in buildings.<sup>74</sup>

### 3.2 Cooling paints

To further simplify the processing of RSC materials and facilitate the application in buildings, worldwide research efforts have been devoted to developing cooling paints, which can be compatible with high-throughput rolling, brushing, spraying

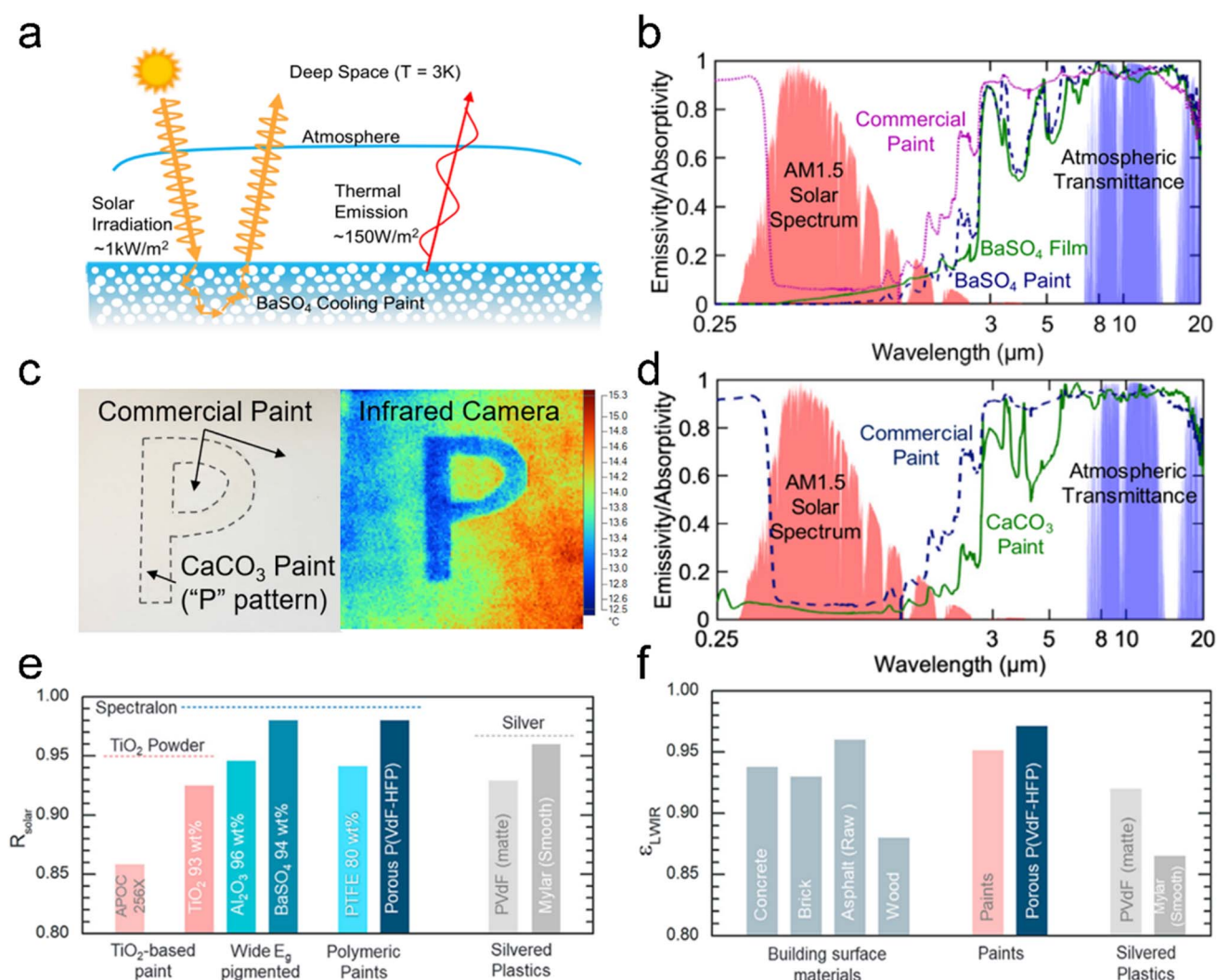


Fig. 4 The recent advance of radiative cooling paints. (a) Schematic of  $\text{BaSO}_4$  cooling paints with heat exchange. (b) The emission and absorption spectral profiles of  $\text{BaSO}_4$  cooling paints. (c) The visible and infrared photographs of  $\text{CaCO}_3$  cooling paints. (d) The emission and absorption spectral profiles of  $\text{CaCO}_3$  cooling paints. (e) The solar reflectance of cooling paints and other cooling materials. (f) The infrared emissivity of building surface materials, paints and silvered plastics. (a and b) Reproduced with permission from ref. 79 Copyright 2021, American Chemical Society. (c and d) Reproduced with permission from ref. 80 Copyright 2020, Elsevier. (e and f) Reproduced with permission from ref. 81 Copyright 2020, Elsevier.

and scraping methods.<sup>75–77</sup> In 2018, Atiganyanun *et al.* introduced the pioneering concept of daytime cooling paints utilizing silica microspheres. These paints exhibit high solar reflectivity of over 97% and infrared emissivity of over 94% resulting in a sub-ambient temperature drop of 12 °C under strong solar radiation.<sup>78</sup> Subsequently, Ruan's group has contributed a lot to developing various cooling paints based on  $\text{CaCO}_3$ ,  $\text{BaSO}_4$  and hBN-acrylic materials, which generally present strong solar reflection and infrared emission (Fig. 4a–d).<sup>79,80,82,83</sup> Moreover, Li and Fan's group also developed various cooling paints based on core-shell particles and rod-like particles, which can enable a high reflectivity of over 95% and infrared emissivity of over 94%, resulting in great cooling performance under strong solar radiation.<sup>84</sup> Additionally, Raman's group revealed that wide-bandgap white particles (*e.g.*,  $\text{BaSO}_4$ ,  $\text{CaCO}_3$  and  $\text{MgO}$ ) have substantial potential in enhancing the solar reflection of cooling paints, which is significantly higher than that of  $\text{TiO}_2$ -based paints and even higher than that of porous cooling coatings (Fig. 4e).<sup>79,80,82</sup> Meanwhile, cooling paints can also present strong infrared emission and effectively dissipate the cooling load in buildings (Fig. 4f).

Moving forward, various strategies have been developed to further enhance the cooling performance of cooling paints. For instance, Xue *et al.* introduced fluorescent particles into cooling paints, which can absorb ultraviolet light and subsequently convert it to the emitted visible light.<sup>85</sup> With this benefit, the developed cooling paints could achieve a sub-ambient temperature drop of 6 °C and a cooling power of 84.2  $\text{W m}^{-2}$ . In addition, hollow spheres (*e.g.*, glass bubbles) can also substantially enhance the performance of cooling paints *via* multiple scattering of solar radiation.<sup>76,86,87</sup> Nie *et al.* introduced glass bubbles into a polymer substrate and found that the solar reflectivity of cooling paints can be significantly improved from 6% to 92% with the increase of glass bubbles.<sup>86</sup> Sun *et al.* also reported that silica-coated glass bubbles are promising cooling paints with a high solar reflectivity of 96% and infrared emissivity of 98%, delivering a sub-ambient temperature drop of 11.1 °C.<sup>88</sup> Moreover, Park *et al.* recently developed promising cooling paints with raspberry-like hollow silica spheres, which can greatly enhance the backscattering of solar radiation, as confirmed by the modeling results (Fig. 5a and b).<sup>89</sup> Compared with smooth hollow spheres, the raspberry-like one can substantially enhance solar reflection, especially in visible and

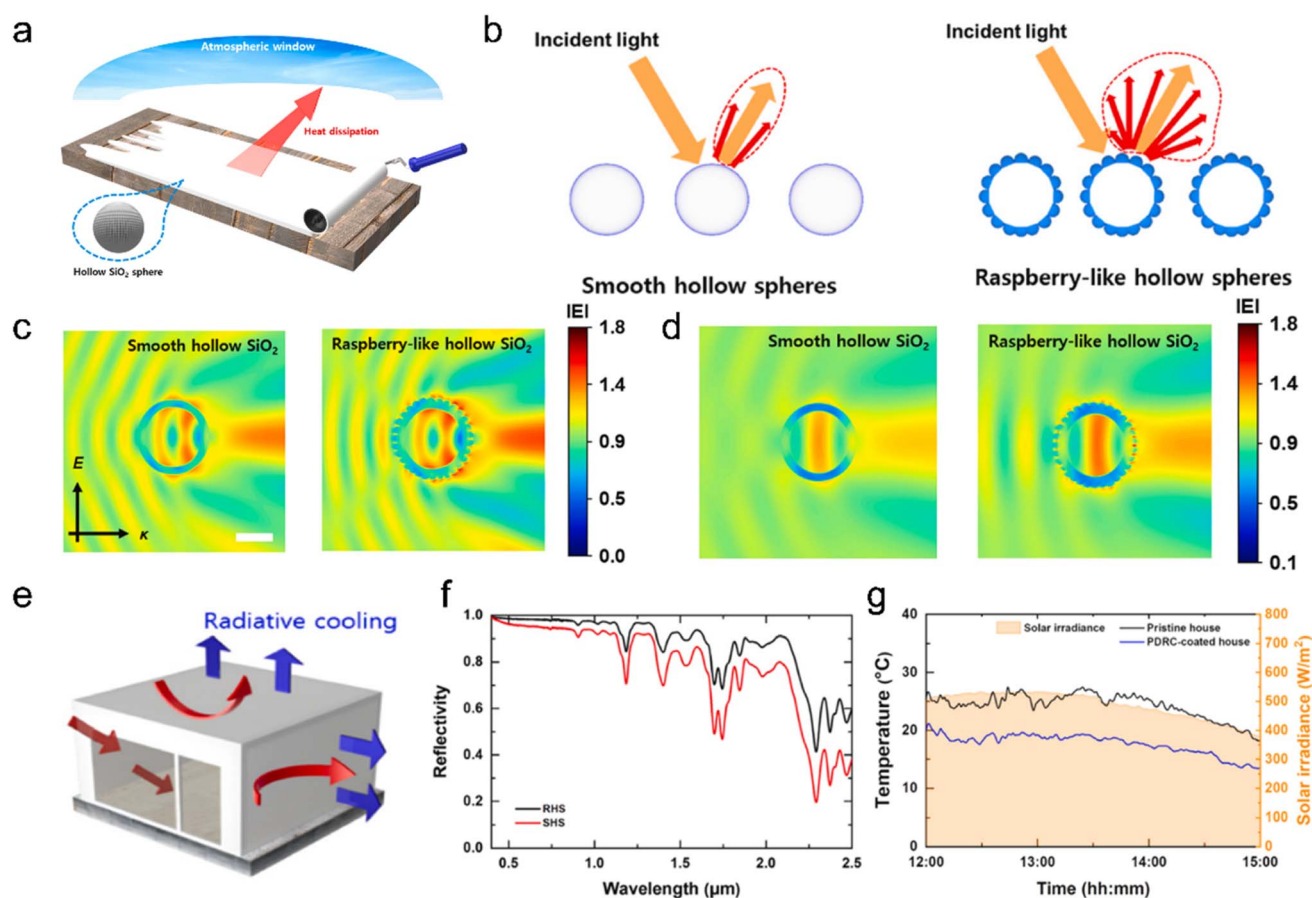


Fig. 5 The radiative cooling paints with hollow spheres. (a) Schematic of radiative cooling paints with hollow spheres. (b) The working mechanism of smooth hollow spheres and raspberry-like hollow spheres for solar scattering. (c and d) Electric field distribution of a single smooth hollow sphere and raspberry-like hollow sphere under 700 nm and 1100 nm wavelengths. (e) Schematic of the heat exchange of house models for radiative cooling applications. (f) The solar reflectance of cooling paints with smooth hollow spheres and raspberry-like hollow spheres. (g) The cooling performance of cooling paints. (a–g) Reproduced with permission from ref. 89 Copyright 2023, Elsevier.

near-infrared bands (Fig. 5c and d). When applied in buildings, the developed cooling paints can reduce the inner temperature by  $\sim 6$  °C (Fig. 5e–g). In addition, Chen *et al.* proposed that breaking glass bubbles by ball milling can enhance the solar reflectivity of cooling paints from 93.3% to 97.3%, which can substantially improve the sub-ambient temperature drop of  $\sim 3.5$  °C in the daytime.<sup>76,87</sup>

From the above discussions, we conclude that porous films prepared by electrostatic spinning, phase separation and phase conversion can provide high-reflectivity solutions utilizing Mie scattering as compared to the use of silver mirrors, which is an important guarantee for large-scale applications in buildings. Notably, the aerogel-based cooling materials have great application potential in building cooling, especially in high-temperature regions throughout the year. Aerogel-based coolers not only achieve superior cooling performance in countering high thermal disturbance in summer, but also block heat intrusion into the indoor environment. Due to the extremely low thermal conductivity, aerogel-based coolers can form a clear temperature gradient from external to internal, which can form an effective thermal insulation for buildings. On the other hand, cooling paints can be processed *via* high-throughput rolling, brushing, spraying and scraping methods, which are favorable for the large-scale applications of this technology in buildings. Nevertheless, the existing cooling paints generally present high thermal conductivity, which may enhance cooling dissipation into the environment.<sup>77,90</sup> The novel concept of “cold-preservation cooling paints” may have application potential in buildings based on the combination of white particles and aerogels.

## 4 Feature functions of radiative cooling materials in buildings

When considering the application of RSC materials in buildings, several critical function design requirements come into play. Firstly, buildings often require cooling materials with multiple colors, necessitating further research in developing sub-ambient RSC materials with a variety of color options. Furthermore, long-term and stable operations are essential for maintaining the optimal cooling performance of buildings over extended periods. Moving forward, to advance the practical applications of the RSC technology, it is highly desirable to develop cooling materials with bifunctionality, capable of providing both cooling and heating capabilities. Additionally, materials with self-adaption properties would be beneficial in adjusting to changing external conditions and optimizing energy efficiency. This section provides a comprehensive summary of recent advancements in functional RSC materials for building applications, covering aspects such as multiple colors, durability, bifunction, and self-adaption.

### 4.1 Colorful cooling materials

From an aesthetic perspective, colorfulness plays a critical role in the selection of RSC materials for building applications. Generally, there are two primary mechanisms to achieve multiple colors in RSC materials: reflection and emission of

specific wavelengths of light. These mechanisms enable the creation of visually appealing RSC materials with a diverse range of colors. The first mechanism involves absorbing the non-target wavelengths of visible light and reflecting the desired wavelength. However, this approach may lead to excessive solar heating and compromised cooling performance. On the other hand, the second mechanism relies on the fluorescent materials that can absorb some solar radiation and convert it into light of different wavelengths. Therefore, fluorescent materials with high photoluminescence quantum yield (PLQY) hold promise as candidates for colorful cooling materials.<sup>91–94</sup> In this section, we provide a summary of recent advancements in the development of colorful RSC materials. Furthermore, we highlight the potential applications of quantum dot materials, which offer a combination of excellent cooling performance and vibrant colors.

**4.1.1 Reflection-based colorful materials.** In the early stage of RSC technology, abundant research efforts were devoted to designing radiative coolers based on photonic structures, which can achieve the flexible modulation of solar radiation and mid-infrared lights.<sup>26,27,29</sup> In the background, some research attempts have been made to develop colorful cooling materials with photonic structures.<sup>95–98</sup> In 2018, Lee *et al.* designed colorful coolers based on thin-film optical resonators, which could present multiple colors, accompanied by a daytime sub-ambient temperature drop of 3.9 °C.<sup>97</sup> Subsequently, Sheng *et al.* also employed a multilayer photonic structure to design colorful radiative coolers, which can deliver a cooling power of 44–52 W m<sup>−2</sup> at ambient temperature.<sup>96</sup> Recently, Cho *et al.* developed TiN/ZnS/Ag coatings with a trilayer structure, which can present a wide color gamut and sub-ambient cooling temperature drop for all magenta, green, cyan and yellow films.<sup>99</sup> Despite the great benefits, the complicated processing and high cost have placed great restrictions on their actual applications in buildings. To counter this issue, some promising strategies have been developed to facilitate produce colorful materials. Ma's group<sup>98</sup> recently developed flexible colorful radiative coolers with interferometric retroreflection based on close-packed polystyrene microspheres on polydimethylsiloxane (PDMS), which could achieve significantly enhanced cooling performance over that of colorful commercial paints under a solar radiation of 1000 W m<sup>−2</sup>. Moreover, Zhao *et al.*<sup>100</sup> developed colorful cooling films based on the composite opal photonic crystal structure, which can reflect the target light to generate the desired color and efficiently scatter the other incident solar radiation, resulting in a sub-ambient cooling of  $\sim 4.1$  °C under strong solar radiation.

Although the above photonic-structure coolers can achieve sub-ambient cooling performance, the actual applications in buildings are currently hindered by challenges related to processing and cost. In 2019, Cui's group developed colorful cooling textiles with the introduction of inorganic nanoparticles (Prussian blue, iron oxide, and silicon) for the coloring component.<sup>32</sup> The developed cooling textiles can all present temperature reduction by  $\sim 1.6$ – $1.8$  °C with clear colors, compared to the commercial counterparts. Subsequently, Yang and Yu's group developed bilayer coatings with a thin and



visible-absorptive top layer for multiple colors and the solar-scattering underlayer for radiative cooling (Fig. 6a–c).<sup>14</sup> Compared with commercial paints, the developed bilayer coatings can achieve a daytime temperature drop of  $\sim 3.0$ – $15.6$  °C for black, red, blue and yellow colors with high purity (Fig. 6d and e). Other pigments have been explored for the development of colorful coolers. However, it is important to note that these pigments typically do not achieve sub-ambient cooling performance under strong solar radiation.<sup>101–103</sup> For instance, Chen *et al.*<sup>103</sup> developed colorful bilayer coatings with plasmonic nanospheres for colors in the top layer and SiO<sub>2</sub> microspheres in the underlayer, which can achieve high solar reflectance and infrared emission, delivering the sub-ambient temperature drop. Moreover, Li and Fan's group recently designed colorful cooling coatings based on a facile solvothermal reaction.<sup>104</sup> Through sacrificing a part of visible reflections, the colorful cooling coatings can achieve sub-ambient cooling performance under strong solar radiation. In addition, Zhu *et al.* employed cellulose nanocrystals to develop cooling coatings, which can

selectively reflect visible light, achieving multiple colors and a high solar reflection of 97%.<sup>105</sup> Nevertheless, radiative coolers with excellent cooling performance often exhibit lighter colors. This phenomenon is primarily attributed to the tradeoff between solar absorption and cooling effectiveness.

**4.1.2 Fluorescence-based colorful materials.** On the other hand, fluorescent materials have been demonstrated to hold great potential for designing high-performance radiative coolers with multiple colors (Fig. 7a and b). Fluorescent materials can absorb solar radiation and subsequently convert it into light of other wavelengths.<sup>106,107</sup> Therefore, fluorescent materials with a high PLQY (*e.g.*, perovskite quantum dots) can significantly reduce the solar absorption of radiative coolers, which can enable superior cooling performance (Fig. 7c and d).<sup>91,92</sup> For instance, Son *et al.* introduced the promising perovskite quantum dots to develop colorful cooling coatings with great cooling performance (Fig. 7b).<sup>91</sup> The developed white, green and red coolers can achieve sub-ambient cooling temperature drops of 4.2, 3.6, and 1.7 °C, respectively, under strong solar radiation.

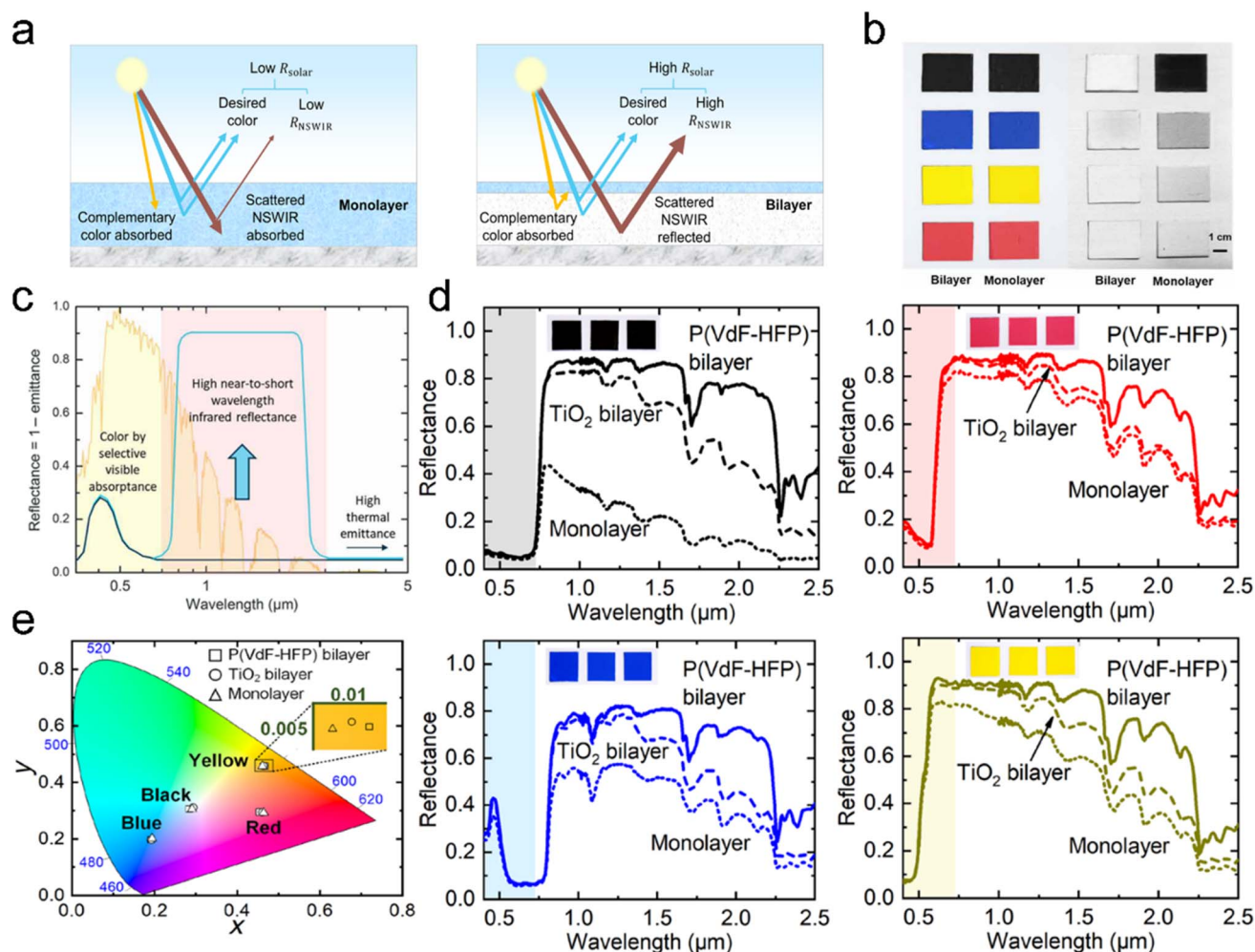


**Fig. 6** The colorful radiative cooling films with pigment particles. (a) Schematic of the thermal exchange with monolayer and bilayer colorful cooling films. (b) The visible and near-to-short infrared photographs of cooling films based on monolayer and bilayer structures. (c) The visible absorption and near-to-short infrared reflection of bilayer colorful cooling films. (d) The solar reflection spectral profile of colorful films. (e) The chromaticity of cooling films with various colors in the CIE 1931 color space. (a–e) Reproduced with permission from ref. 14 Copyright 2020 AAAS.

The group<sup>94</sup> further fabricated colorful cooling coatings based on Cu-based quantum dots, which can enable the light emission of yellow, red and brown colors, resulting in great cooling performance. Recently, Zhu's group designed colorful radiative coolers with perovskite quantum dots based on electrostatic-spinning/inkjet printing methods (Fig. 7e–g).<sup>92</sup> The promising green, yellow and red coolers can achieve a sub-ambient temperature drop of 5.4–2.2 °C under direct solar radiation, indicating their great application potential in buildings.

It can be confirmed from the above discussions that quantum dot fluorescent materials are promising candidates for the development of radiative cooling materials, especially for cooling paints. Quantum dot-based cooling paints can not only enable great cooling performance, but also present multiple colors for building applications. Nevertheless, the stability issues still places some restrictions on their actual applications, especially for lead, cadmium, and perovskite-based quantum dots, which are not stable in the environment

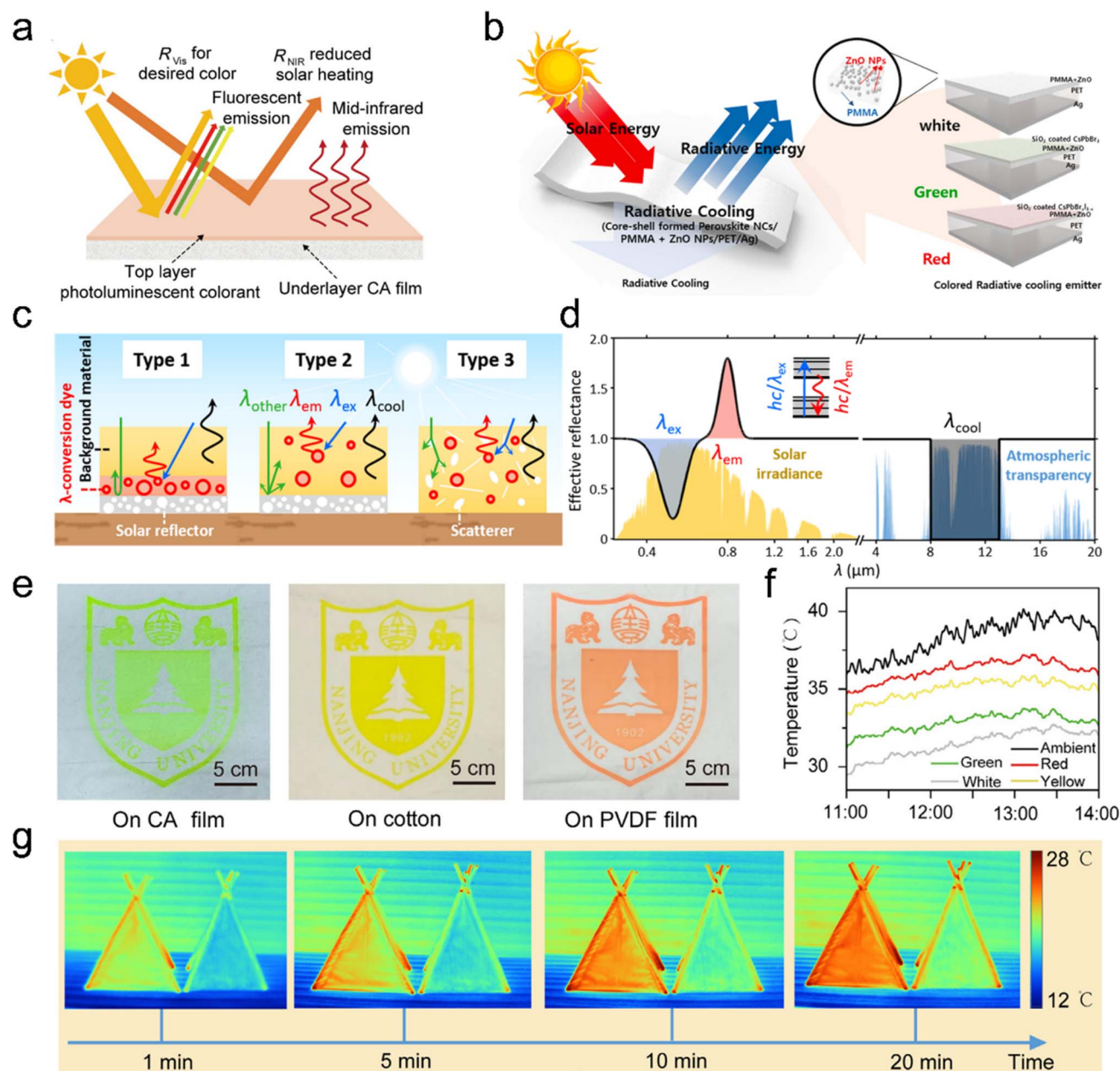


Fig. 7 The colorful radiative cooling coatings with quantum dot particles. (a) Schematic of thermal exchange with colorful cooling coatings with a bilayer structure. (b) Schematic of thermal exchange with cooling coatings with various colors. (c) The working mechanism of cooling coatings with wavelength conversion for various structures. (d) The spectral profiles of effective reflectance of colorful cooling coatings with wavelength conversion. (e) Optical photographs of logos with various colors. (f) The performance of colorful radiative cooling coatings. (g) Infrared photographs of a green tent with commercial coatings and quantum dot-based cooling coatings. (a and e–g) Reproduced with permission from ref. 92 Copyright 2022, Elsevier. (b) Reproduced with permission from ref. 91 Copyright 2021, Elsevier. (c and d) Reproduced with permission from ref. 106 Copyright 2022, American Chemical Society.

with water and oxygen.<sup>108–113</sup> Moreover, the structure of quantum dots may also be destroyed by high-energy ultraviolet radiation, which may accelerate the degradation of colorful paints. The epitaxial growth of silica shell can partly solve this problem, but the size homogeneity of quantum dots may be reduced with this strategy, resulting in impure colors for cooling paints.<sup>91,92</sup> Therefore, more research efforts should be devoted to further addressing the stability issue of quantum dot materials.

#### 4.2 Durability of cooling materials

For cooling materials intended for building applications, durability is a critical factor to consider.<sup>114–116</sup> Generally, building integrated materials are faced with a harsh working environment, *e.g.*, oxidation, water erosion and ultraviolet damage. For instance, most organic cooling materials may be destroyed after long-term exposure to solar radiation.<sup>117–119</sup> Moreover, the widely used titanium dioxide-based paints will also be damaged after the absorption of high-energy ultraviolet light, resulting in inevitable photocatalytic degradation.<sup>81</sup> In this section, the recent advancements of durable RSC materials are systematically summarized focusing on their potential as promising candidates for building applications.

Weather resistance is highly important for the actual operation of RSC materials. In 2021, Wang *et al.*<sup>120</sup> developed porous

films with an ethylene–propylene–diene copolymer and SiO<sub>2</sub> particles, resulting in great cooling performance and super-hydrophobic self-cleaning function. After ultraviolet exposure and chemical immersion with different pH values, the porous cooling films presented similar cooling temperature drop to that of original films. Subsequently, Luo *et al.* developed porous cooling films *via* photopolymerization-induced phase separation, which can enable strong solar reflection and infrared emission.<sup>121</sup> Moreover, the developed cooling films presented excellent resistance to long-term ultraviolet exposure, high temperature and chemicals. After exposure to ultraviolet light at high humidity for 50 days, the appearance, microstructure and spectral profiles showed nearly no change, indicating the great stability of cooling films.

In addition, Zhu's group systematically investigated the durability of nanocomposite polymers, which presented superior cooling performance and improved mechanical properties (Fig. 8a).<sup>119</sup> More importantly, the developed nanocomposite coolers showed significantly enhanced resistance to high-energy ultraviolet lights *via* the absorption by K<sub>2</sub>Ti<sub>6</sub>O<sub>13</sub>. Compared to ordinary poly(ethylene oxide) (PEO) coolers, the mechanical properties and ultraviolet resistance were improved by 7 and 12 times, respectively (Fig. 8b and c). With these benefits, solar reflectance and appearance remained nearly unchanged after the continuous aging test for 720 h under

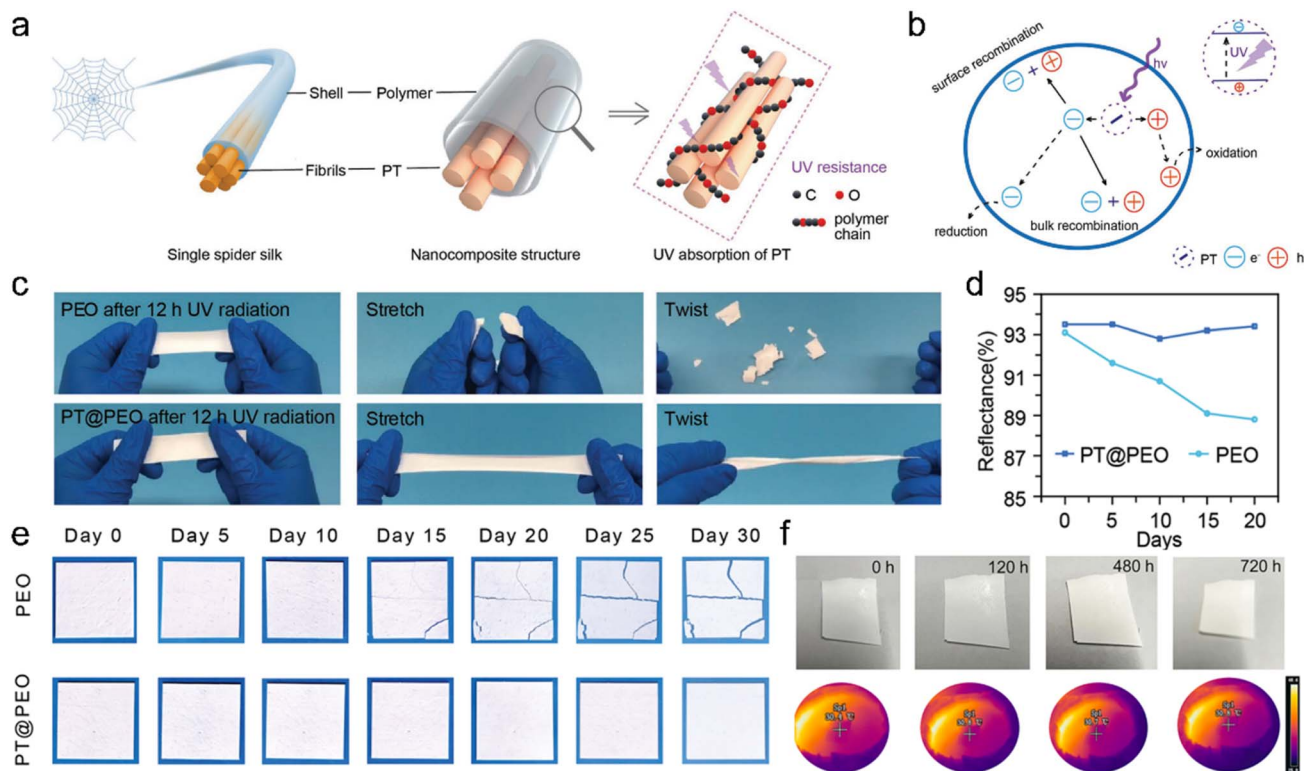


Fig. 8 The radiative cooling films with anti-ultraviolet function. (a) Schematic of the design of the spider-silk-inspired nanocomposite. (b) Schematic of the working mechanism of the PEO cooling films with ultraviolet stability. (c) The photograph of stability experiments for two cooling films after 12 h ultraviolet radiation. (d) The evolution of solar reflectance under the outdoor placement. (e) The photograph of two cooling films under the outdoor placement. (f) The visible and infrared photographs of the developed porous cooling films under the continuous ultraviolet illumination. (a–e) Reproduced with permission from ref. 119 Copyright 2022, Wiley. (f) Reproduced with permission from ref. 118 Copyright 2023, Elsevier.



outdoor solar radiation (Fig. 8d and e). Moreover, Cai *et al.* developed porous cellulose composite films with a hierarchical micro/nanostructure, which can enable optical and mechanical properties, and anti-ultraviolet function.<sup>118</sup> With these benefits, the cooling films presented a high solar reflectivity of 97.6% and mechanical properties enhanced by 13 times. After the continuous ultraviolet aging test for 720 h, the solar reflectivity of cellulose-based cooling films remained nearly constant, indicating great working stability under strong solar radiation (Fig. 8f).

Besides porous coolers, cooling paints have been demonstrated to hold great application potential in buildings. For instance, Yang's group<sup>54</sup> developed stable cooling paints with the uniform micro-assembly of poly(vinylidene fluoride-co-hexafluoropropene) nanoparticles, which can improve solar back-scattering and enhance the corresponding cooling performance. Moreover, the developed cooling paints presented the stability of storage and processability to yield uniform

coatings with no cracks. The spectral profiles of cooling coatings for solar reflection undergo minor changes after ultraviolet exposure of 12 days and aging at the temperature of 80 °C and relative humidity of 70% for 10 days. Moreover, Feng *et al.*<sup>122</sup> developed inorganic radiative coolers based on super-amphiphobic SiO<sub>2</sub> nanoparticles, which exhibited enhanced solar reflectivity and thermal emissivity with super-hydrophobicity function (water contact angle >158° and oil contact angle >151°). The super-hydrophobic surface help films avoid over 7.5 °C increase of temperature under the solar radiation of 1500 W m<sup>-2</sup> after being immersed by oil pollution. To counter the effect of natural soiling and ultraviolet radiation on radiative coolers, Song *et al.*<sup>117</sup> employed titanium dioxide (TiO<sub>2</sub>) nanoparticles with hierarchical porous morphology based on an evaporation-driven assembly, which can simultaneously enable strong solar reflection and effective anti-aging function (Fig. 9a–c). With the strategy, the solar reflection of the developed paints was only reduced by ~0.4% and 0.5% after

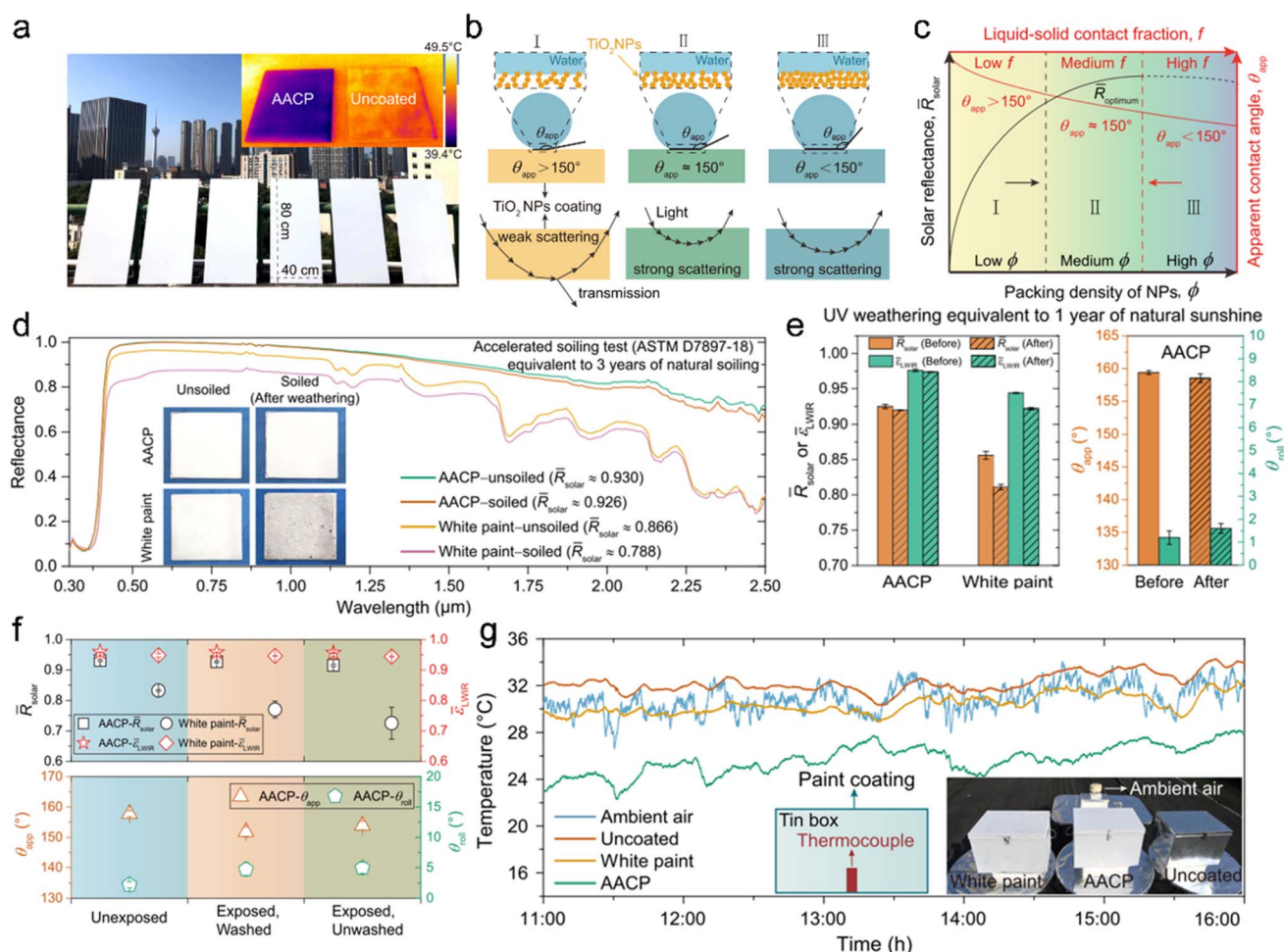


**Fig. 9** The durable radiative cooling materials. (a) The visible and infrared photographs of cooling coatings based on titanium dioxide (TiO<sub>2</sub>) nanoparticles with a porous structure. (b) Schematic of the working mechanism of TiO<sub>2</sub>-based porous cooling coatings. (c) The function of solar reflection and packing density of TiO<sub>2</sub>-based porous cooling coatings. (d) The solar reflection of the developed cooling coatings after soiled/unsoiled treatments. (e) The variation of solar reflection, infrared emissivity and wetting properties of the developed cooling coatings after 1000 h of ultraviolet exposure. (f) The optical and wetting properties of the developed cooling coatings after outdoor exposure for 6 months. (g) The cooling performance of the developed cooling coatings and the control coatings. (a–g) Reproduced with permission from ref. 117 Copyright 2022 Springer Nature.

the simulated natural soiling of 3 years and simulated solar radiation of 1 year (Fig. 9d). Moreover, the cooling performance could remain nearly constant after aging for 6 months under real-world conditions (Fig. 9g).

Despite significant advancements in developing durable cooling materials, there are still notable shortcomings in terms of cooling performance, stability and the lack of unified evaluation standards for various RSC materials. These factors currently impose significant restrictions on their practical applications in buildings. Therefore, the establishment of unified standards for evaluating the durability of RSC materials, especially paints used in buildings, is highly encouraged. With worldwide efforts, it can be expected that the gap between laboratory results and applications of cooling materials will be gradually narrowing. Recently, Hu's group developed a promising solution-processed radiative cooling glass, which can present a sub-ambient temperature drop of  $\sim 4$  °C under high-humidity conditions (up to 80%).<sup>18</sup> Moreover, the cooling glass can maintain high

solar reflectance under harsh conditions, including water, ultraviolet light, soiling and high temperature. Moving forward, more research efforts are encouraged to perform the pilot applications of cooling materials in buildings, which can significantly advance the progress of RSC technology.

### 4.3 Bifunctional materials

It is well accepted that RSC technology can be directly applied in hot weather regions throughout the year (e.g., Singapore) without causing any negative impact.<sup>51</sup> Nevertheless, the vast majority of population is distributed in mid-latitude regions, which also have a great cooling demand in summer to counter the increasingly severe global warming and extreme weather. The direct applications of cooling materials in buildings will substantially enhance the heat energy consumption in the winters of these regions, greatly blocking the actual applications of this technology. To address this tough issue, abundant

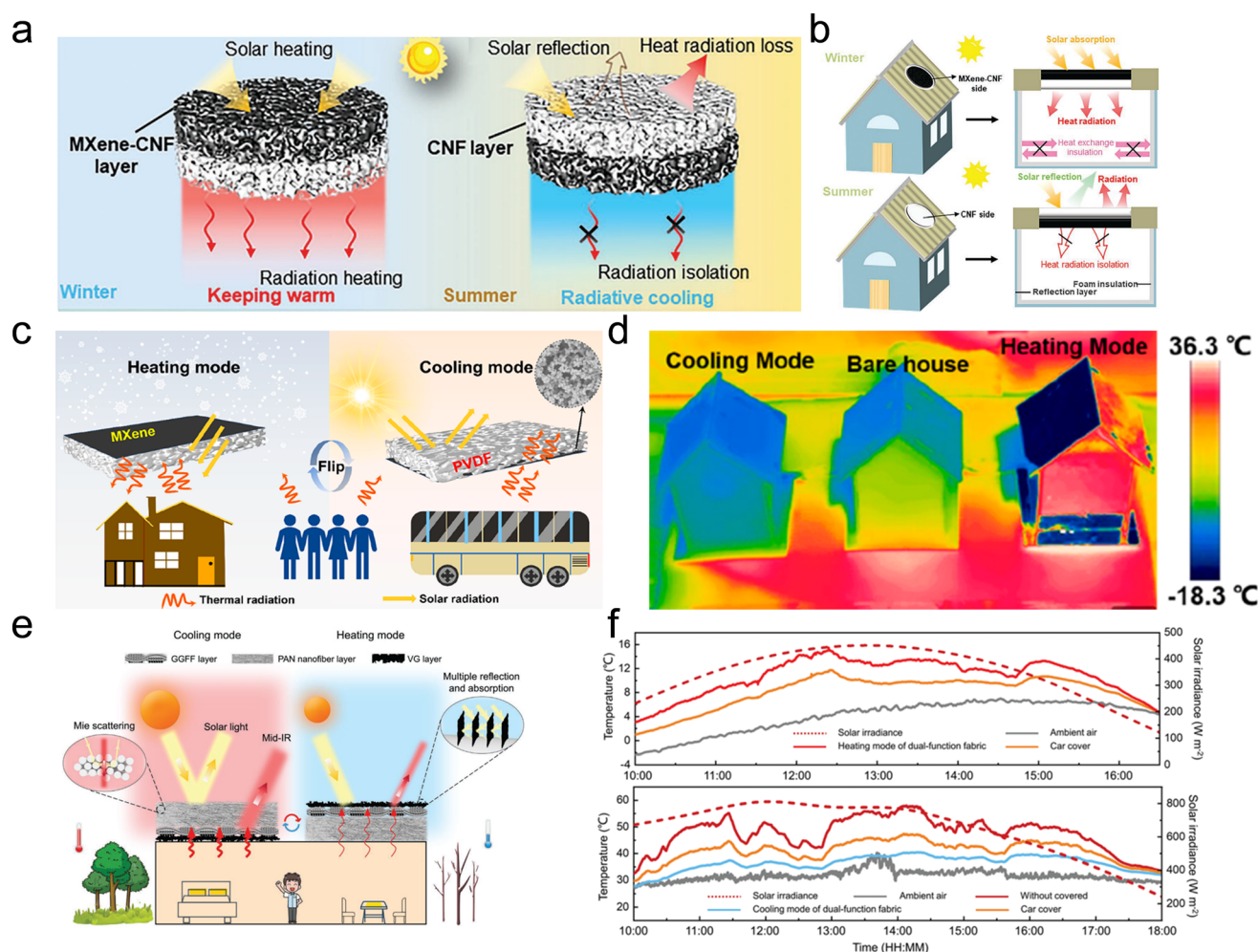


Fig. 10 The promising bifunctional materials. (a) Schematic of bifunctional materials with Janus MXene-nanofibril aerogels. (b) Schematic of the applications and thermal exchange process of bifunctional materials in winter and summer. (c) Schematic of bifunctional materials with MXene-PVDF materials. (d) The infrared photographs of building models with bifunctional materials. (e) Schematic of bifunctional materials for solar heating and radiative cooling. (f) The heating and cooling performance of bifunctional materials. (a and b) Reproduced with permission from ref. 127 Copyright 2023 Wiley. (c and d) Reproduced with permission from ref. 124 Copyright 2023 American Chemical Society. (e and f) Reproduced with permission from ref. 128 Copyright 2023 Wiley.

research efforts have been devoted to developing cooling and heating bifunctional materials for building applications.

**4.3.1 Unswitchable bifunctional materials.** Abundant research efforts have been devoted to developing bifunctional materials for buildings.<sup>123–126</sup> For instance, Yang *et al.* designed bifunctional MXene–nanofibril aerogels, which achieved remarkable thermal regulation in both hot and cold environments (Fig. 10a and b).<sup>127</sup> When employed in building roofs, the developed aerogels can effectively reduce the indoor temperature to below 30 °C in summer and maintain the temperature above 25 °C in winter, which will greatly reduce cooling and heating energy consumption throughout the year. In addition, Shi *et al.*<sup>124</sup> developed bifunctional porous films with MXene in porous poly(vinylidene fluoride) for the simultaneous implementation of solar heating and radiative cooling (Fig. 10c and d). In cooling mode, the developed films presented a high solar reflectivity of 96.7% and infrared emissivity of 96.1%, resulting in a sub-ambient temperature drop of 9.8 °C in the daytime. In heating mode, the film achieved a high solar absorptivity of 75.7% and low infrared emissivity of 11.6%, resulting in the heating temperature rise of 8.1 °C.

Preliminary attempts have been made to explore the potential of bifunctional films in direct building applications, with focus on building energy savings. These efforts have yielded promising results and demonstrated the effectiveness of bifunctional films in improving energy efficiency in buildings. For instance, our group developed bifunctional modules with the coupling of radiative cooling and solar heating, which can be switched *via* flexible flipping.<sup>5</sup> The developed modules can maintain the indoor temperature below 27.5 °C in summer and around 25 °C during the daytime in winter. This allows for a significant energy-saving rate of 42.4% in buildings, highlighting the potential of bifunctional films in reducing energy consumption. Subsequently, Yang *et al.* developed bifunctional films that could achieve the switch of heating and cooling *via* louver structures.<sup>129</sup> The modeling results showed that the dynamic converting structures could achieve an energy saving of ~746 GJ and the corresponding carbon dioxide emission reduction of ~147 tons. Recently, Yuan *et al.* developed heating and cooling bifunctional films for building energy saving (Fig. 10e and f).<sup>128</sup> The modeling results revealed that the developed bifunctional films can enable the great annual energy saving of ~15.5–31.1 MJ (m<sup>2</sup> per years) over that of cooling-only or heating-only films.

**4.3.2 Switchable bifunctional materials.** Nevertheless, the switch of cooling and heating sides is still not convenient for building applications. Stimulus-driven materials offer promising routes for the building applications of bifunctional films. For instance, Yang's group developed porous polymer coatings with optical transmittance transition through the reversible wetting of common liquids (Fig. 11a and b).<sup>131</sup> For the regulation of solar radiation, porous poly(vinylidene fluoride-*co*-hexafluoropropene) presented a substantial change of solar transmittance from 20% to 94% upon the wetting of isopropanol, resulting in a sharp temperature transition from ~40 to ~60 °C (Fig. 11c and d). Moreover, polyethylene porous films can also achieve a great change of mid-infrared transmittance

from 0.3% to 64% with the introduction of alcohols, which can enable the temperature switch from sub-ambient temperature to ~55 °C. Subsequently, Fei *et al.*<sup>123</sup> also reported monolayer porous coating with fast switch from a high solar reflection of 96.6% to a high solar transmittance of 86.6%, which can greatly modulate the indoor temperature of buildings based on solar heating and radiative cooling. Moreover, Feng and Wang's group reported that bacterial celluloses also have a similar switch of solar transmittance upon wetting, which can enable significant temperature regulation in summer or winter.<sup>130</sup> In addition, Zhao *et al.*<sup>132</sup> reported that the solar transmittance of silicone coatings can also be reversibly modulated with stress stimulus, which can enable a sub-ambient temperature drop of ~5 °C in a hot environment and temperature rise from ~10 to 28 °C in a cold environment.

Despite the benefits, the stimulus of the solvent and stress is not still convenient and practical for the actual applications of bifunctional films in buildings. Li *et al.*<sup>28</sup> developed a dual-mode device integrated solar heating and radiative cooling based on a facile electrostatically controlled thermal contact (Fig. 11e–g). In a hot environment, radiative cooling films are attached on building roofs and can achieve a cooling power of 71.6 W m<sup>−2</sup> for indoor cooling. In a cold environment, high absorption of solar radiation can provide the heating power density of 643.4 W m<sup>−2</sup> for buildings. Additionally, Zhao *et al.* also developed a dual-mode glazing device with the great regulation of solar transmittance *via* applied voltage.<sup>133</sup> In cooling mode, the devices can work as radiative coolers with the cooling power of 20–60 W m<sup>−2</sup> under the solar radiation of 560–970 W m<sup>−2</sup> in summer. In the heating mode, high solar transmittance can enable a great heating power of over 400 W m<sup>−2</sup> in winter. With these benefits, the dual-mode devices can reduce the annual heating/cooling energy consumption by ~23% in buildings.

In addition, the switch of bifunctional materials with solar heating and radiative cooling can also be fulfilled *via* temperature-sensitive actuating films. Ma's group<sup>134</sup> recently proposed that the temperature-sensitive actuation can enable the functional transition of radiative cooling and solar heating with the variation of ambient temperature, which can deliver an average heating power of ~859.8 W m<sup>−2</sup> or a cooling power of ~126.0 W m<sup>−2</sup>. Moreover, the group further proposed that the above structure can be further employed to simultaneously modulate the optical properties of bifunctional materials in the two wavelength ranges (solar radiation and mid-infrared lights).<sup>135</sup> With the introduction of thermochromic powders, the developed bifunctional films can enable the high absorption of visible light (~73%) and low emissivity of mid-infrared light (~28%) in heating mode, while the visible-light reflectivity and infrared emissivity reach ~65% and ~95%, respectively in cooling mode. However, the applications of temperature-sensitive actuating films may face some critical issues in buildings, *e.g.*, complexity, reliability, and safety.

These examples illustrate the potential of stimulus-driven materials in bifunctional films for building applications. By leveraging the reversible responses of these materials to external stimuli such as wetting or stress, it becomes possible to



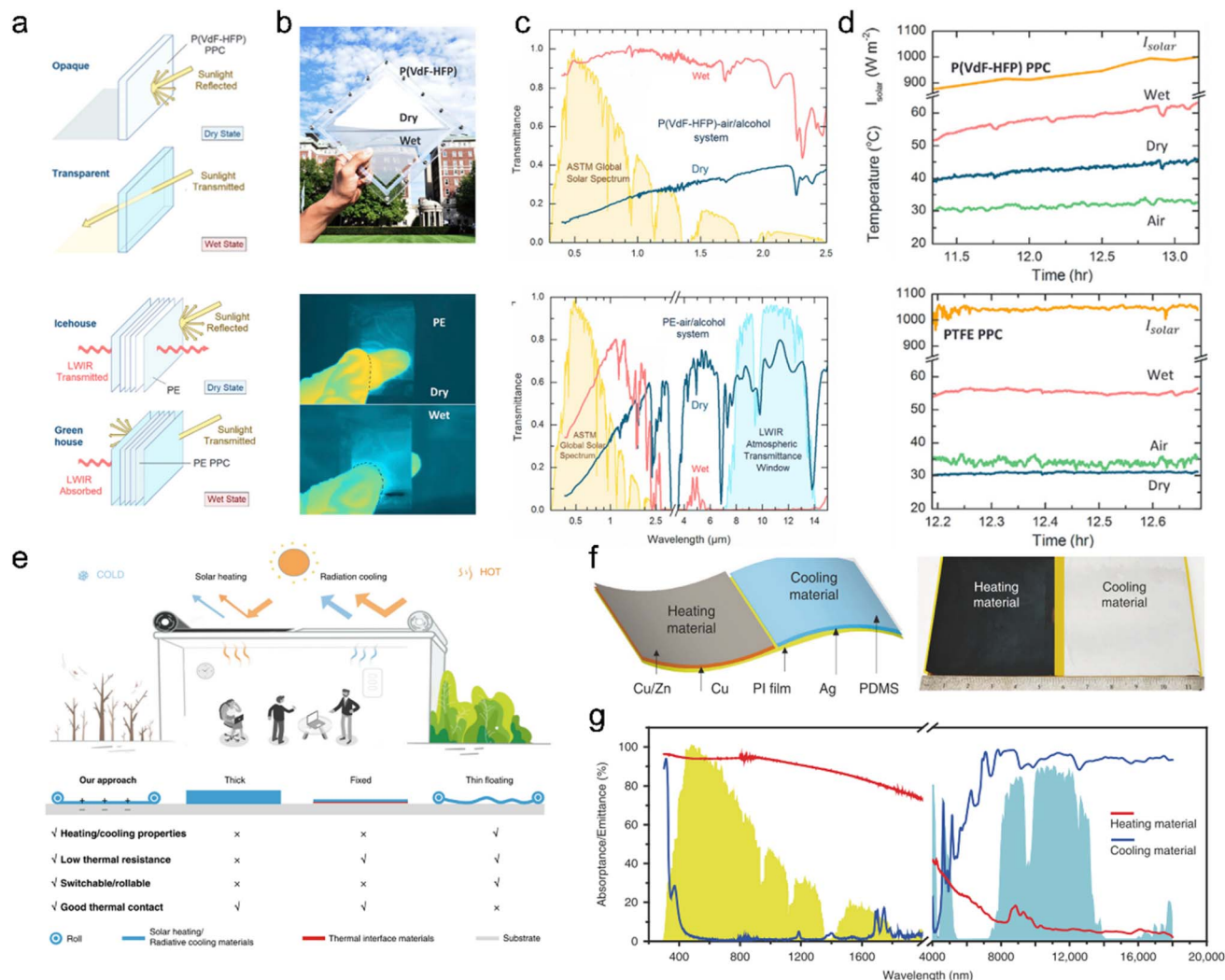


**Fig. 11** The switchable design of bifunctional materials. (a) Schematic of the switching of the porous polymer cooler with the solvent. (b) The visible and infrared photographs of two porous polymer coolers in dry and wet states. (c) The spectral profiles of two porous polymer coolers in dry and wet states. (d) The temperature control performance of two porous polymer coolers in dry and wet states. (e) Schematic of the dual-mode strategies in heating and cooling modes. (f) Schematic and photograph of dual-mode films. (g) The spectral profiles of bifunctional films in heating and cooling modes. (a–d) Reproduced with permission from ref. 130 Copyright 2019 Elsevier. (e–g) Reproduced with permission from ref. 28 Copyright 2020 Springer Nature.

achieve efficient and controlled switching between cooling and heating modes, thereby enhancing energy efficiency and thermal comfort in buildings. Continued research and development in this area will further advance the practical implementation of stimulus-driven materials for building energy-saving strategies.

However, there are critical issues that currently hinder their widespread adoption in building applications, including integrated methods and cost considerations. One major challenge is the lack of facile switching between cooling and heating sides in most bifunctional films. Electrostatically controlled methods,<sup>28</sup> for instance, restrict the cooling and heating materials to specific areas, leading to non-uniform cooling or heating within an indoor environment and poor thermal comfort. Another obstacle is the high cost associated with applied-voltage control,<sup>133</sup> particularly when utilizing indium tin oxide

(ITO) glass. This cost factor imposes restrictions on the large-scale implementation of bifunctional materials in buildings, especially for applications such as glass curtain walls. Furthermore, the reliability and safety of the temperature-sensitive actuating strategy need to be addressed before their direct applications in buildings. To overcome these challenges, it is imperative to encourage further research efforts aimed at developing facile and cost-effective control strategies for the application of bifunctional materials in buildings. This may involve exploring alternative control mechanisms, optimizing manufacturing processes to reduce costs, and conducting rigorous testing and validation to ensure reliability and safety.

#### 4.4 Adaptive cooling materials

For the building applications of cooling materials, the main goal is to provide additional cooling power to control indoor

temperature for cooling load removal. Considering human comfort and building energy saving, indoor temperature should be controlled within suitable range, which requires more energy consumption from cooling and heating. Developing temperature-dependent self-adaptive cooling materials is one of the promising routes to address this issue.<sup>136–138</sup> In this section, we provide detailed discussions on temperature-dependent self-adaptive cooling materials and highlight their promising application potential in buildings.

**4.4.1 VO<sub>2</sub>-based adaptive materials.** Temperature-dependent self-adaptive cooling materials are designed to exhibit specific cooling properties that vary with temperature changes. These materials can automatically adjust their cooling performance based on the surrounding temperature, providing enhanced control over indoor thermal conditions. By dynamically responding to temperature fluctuations, they enable more efficient and targeted cooling, minimizing energy waste and optimizing human comfort. For the modulation of mid-infrared emission, vanadium dioxide (VO<sub>2</sub>) materials have been demonstrated to hold great potential in fulfilling self-adaptive function.<sup>139–141</sup> Generally, VO<sub>2</sub> materials experience the semiconductor-to-metal phase transition with temperature rise to the critical temperature of ~68 °C. More specially, VO<sub>2</sub> presents a high-emission semiconductor state at a low working temperature, while it converts to low-emission metal state at high temperature.<sup>142,143</sup> This promising property can be employed in simultaneously harvesting solar heating and radiative cooling from the outer space. Recently, Pei's group proposed that VO<sub>2</sub> can be employed to develop a self-adaptive solar absorber/radiative cooler for continuous energy harvesting.<sup>143</sup> In the daytime, solar heating causes VO<sub>2</sub>-based multilayered films to exceed the threshold temperature of 68 °C and enable low infrared emissivity, resulting in the continuously increasing temperature of the solar absorber. In the nighttime, low ambient temperature delivers the strong infrared emission of VO<sub>2</sub>-based films, which can enable a sub-ambient temperature drop for cooling applications. In the vacuum chamber, the developed multilayered films can achieve the temperature rise of over 170 °C in the daytime and a temperature drop of over 20 °C in the nighttime.<sup>142</sup> Similarly, the utilization of VO<sub>2</sub>-based films can facilitate a sub-ambient temperature reduction of approximately 5 °C and a cooling power of approximately 25 W m<sup>-2</sup> during nighttime when used in conjunction with conventional radiative cooling devices.

Nevertheless, this intrinsic property of VO<sub>2</sub> materials is not favorable for the practical applications of temperature regulation within buildings. These challenges can be addressed through the design of a Fabry–Pérot cavity and the modulation of the transition temperature of VO<sub>2</sub> materials *via* tungsten doping, which can reduce the temperature to favorable values.<sup>20,31</sup> In 2021, Wu's group developed mechanically flexible self-adaptive coatings based on tungsten-doped VO<sub>2</sub> with a Fabry–Pérot cavity.<sup>144</sup> The developed self-adaptive coatings presented a low infrared emissivity of ~20% at an ambient temperature lower than 15 °C and a high infrared emissivity of 90% with increase in the ambient temperature to 30 °C, which can substantially reduce the energy consumption for the

cooling/heating of buildings (Fig. 12a). Recently, the group further developed printable and colorful self-adaptive cooling films based on tungsten-doped VO<sub>2</sub> materials *via* roll-to-roll fabrication.<sup>31</sup> The developed self-adaptive films presented emissivity switch from 25% to 85% with increase in the temperature to the transition temperature. Accordingly, the self-adaptive films can enable year-round energy saving or thermal comfort of building applications.

In addition, VO<sub>2</sub> materials also have significant application potential in smart windows for the modulation of mid-infrared emission. For instance, Wang *et al.*<sup>20</sup> designed scalable smart windows based on the structure of VO<sub>2</sub>/PMMA spacer/low-E coating/glass/low-E coating, which could achieve a high infrared emissivity of 61% in a hot environment and low infrared emissivity of 21% in a cold environment (Fig. 12b and d). Moreover, the VO<sub>2</sub>/glass structure can achieve high near-infrared transmittance in a cold environment, effectively increasing the indoor temperature of buildings. In a hot environment, the developed VO<sub>2</sub> films achieved low near-infrared transmittance, reducing the impact of solar heating on buildings. This mechanism can also be combined with electrochromic structures to enhance the modulation of near-infrared lights in promising smart windows. For instance, Sheng *et al.*<sup>145</sup> proposed a co-assembly strategy to develop electrochromic and thermochromic smart windows for building applications. These reduced the transmittance of near-infrared lights by 90% and resulted in a cooling temperature drop of 5 °C under one-sun irradiation (Fig. 12e and f).

**4.4.2 Hydrogel-based adaptive materials.** Solar radiation has a significant impact on the temperature regulation of buildings. Controlling the transmittance of solar energy through transparent windows or curtain walls allows for effective management of energy input and output. The widely used metallized glasses can partly reduce the solar transmittance and therefore alleviate the solar heating effect on an indoor environment in summer.<sup>146</sup> However, the low transmittance of visible and near-infrared lights compromises the favorable solar heating on buildings in winter. To counter this issue, abundant research efforts have been devoted to developing temperature-dependent self-adaptive materials for the modulation of solar transmittance. The thermochromic poly(*N*-isopropylacrylamide) (pNIPAm) hydrogels present high solar transmittance in a cold environment and low solar transmittance with the temperature rise to over the critical temperature (Fig. 13a–c).<sup>136,138,148,149</sup> Accordingly, pNIPAm-based films can maintain a stable working temperature under the great fluctuations of ambient temperature.<sup>147</sup> Moreover, Xu *et al.*<sup>138</sup> revealed that the critical temperature of thermochromic hydrogels can be significantly modulated *via* the introduction of sodium dodecyl sulfate micelles or the hydrophilic monomer *N,N*-dimethylacrylamide, which can broaden the temperature regulation range for building applications. In addition, the mid-infrared emissivity of thermochromic hydrogels can be significantly enhanced with the introduction of polyvinylidene fluoride or graphite, which can enable promising radiative cooling performance.<sup>136</sup>

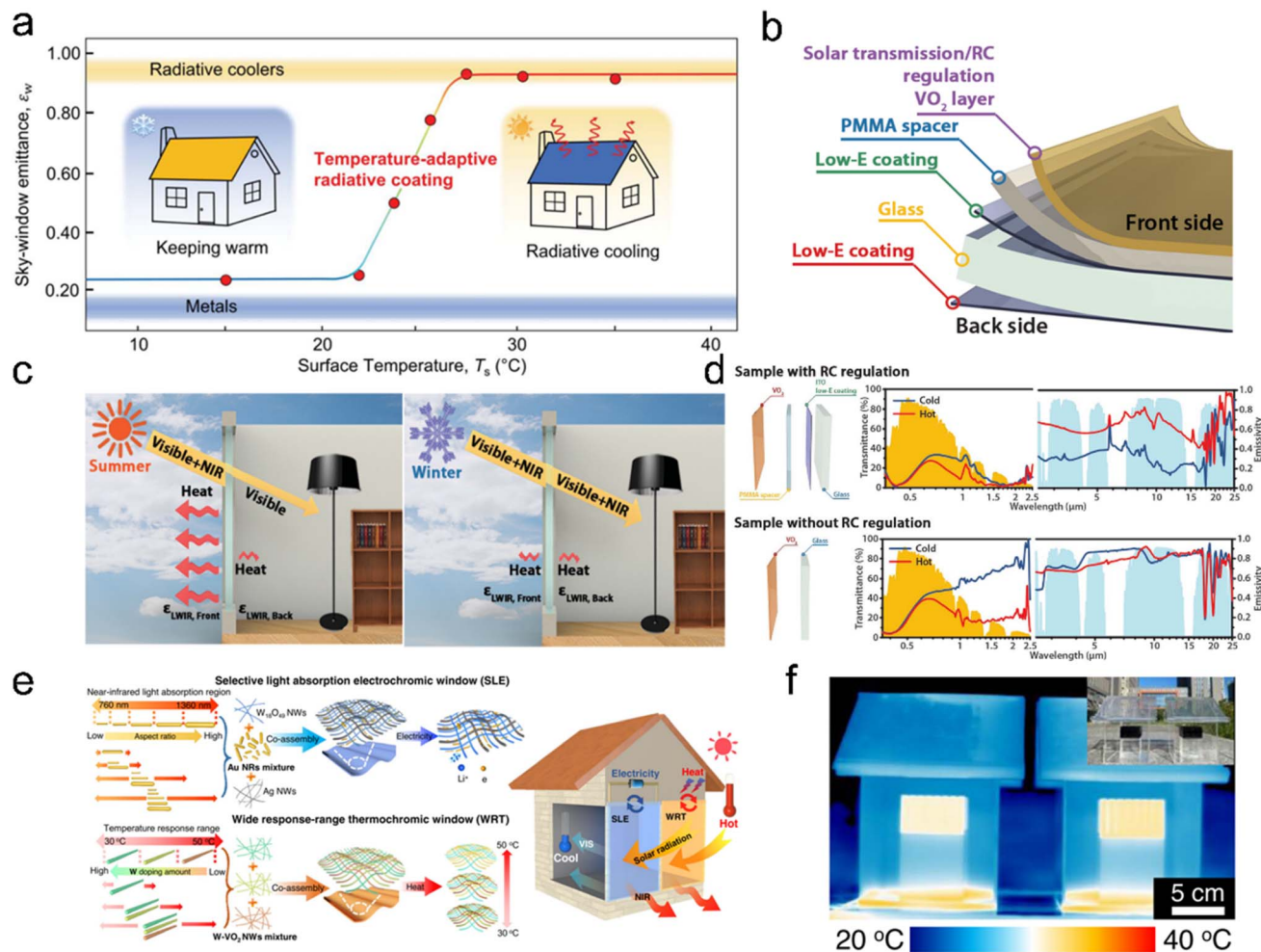


**Fig. 12** The adaptive cooling materials for building applications. (a) Schematic of the switching of infrared emissivity based on thermochromic VO<sub>2</sub> for summer cooling and winter warming. (b) Schematic of the adaptive cooling window based on thermochromic VO<sub>2</sub>. (c) The working mechanism of the adaptive cooling window in summer and winter. (d) The spectral profiles of the adaptive cooling window at heating and cooling modes for two structures. (e) Schematic for the fabrication and working mechanism of electrochromic and thermochromic windows. (f) The infrared photograph of model buildings with two smart windows. (a) Reproduced with permission from ref. 19 Copyright 2021 Springer Nature. (c and d) Reproduced with permission from ref. 20 Copyright 2021 Springer Nature. (e and f) Reproduced with permission from ref. 145 Copyright 2023 Springer Nature.

From the above discussions, it is evident that VO<sub>2</sub> and thermochromic hydrogels have the potential to achieve self-adaptive temperature regulation in the mid-infrared and solar spectral ranges. Combination of these two thermochromic materials can enable simultaneous modulation of solar and mid-infrared lights. For instance, Zhang *et al.*<sup>150</sup> developed dual-band thermochromic films based on VO<sub>2</sub>-PMMA/PMMA spacer/low-E coating/thermochromic hydrogel/low-E coating structures. Accordingly, these developed dual-band self-adaptive films presented high solar transmittance and low infrared emissivity in a cold environment, transitioning to low solar transmittance and high infrared emissivity with temperature rise. However, these self-adaptive films only achieved limited regulation of solar radiation (~20%), indicating their restricted application potential. In addition, Huang's group<sup>13</sup> recently designed promising dual-band self-adaptive films based on pNIPAm/silver nanowire structures. These films demonstrate a solar modulation of 58.4% and mid-infrared modulation of

57.1% (Fig. 13d and e). In a cold environment, self-adaptive films achieve a high solar transmittance of ~65.5% and mid-infrared reflectance of ~64.8%, while these values decreased to ~7.1% and 7.7%, respectively, with increasing ambient temperature. This capacity enables higher energy savings compared to low-E glass and thermochromic hydrogel (Fig. 13f and g).

Despite the significant advancements in self-adaptive materials, there still exist critical issues that limit their practical applications in buildings. Generally, the promising VO<sub>2</sub> materials have huge application potential in smart windows *via* the switch of mid-infrared emissivity. Nevertheless, the high cost and complicated processing methods have placed some restrictions on their applications in building envelopes.<sup>140,141</sup> In addition, thermochromic hydrogels generally have low-cost and facile processing, which are favorable for their applications. However, the low stability of thermochromic hydrogels under strong solar radiation greatly blocks the actual applications,



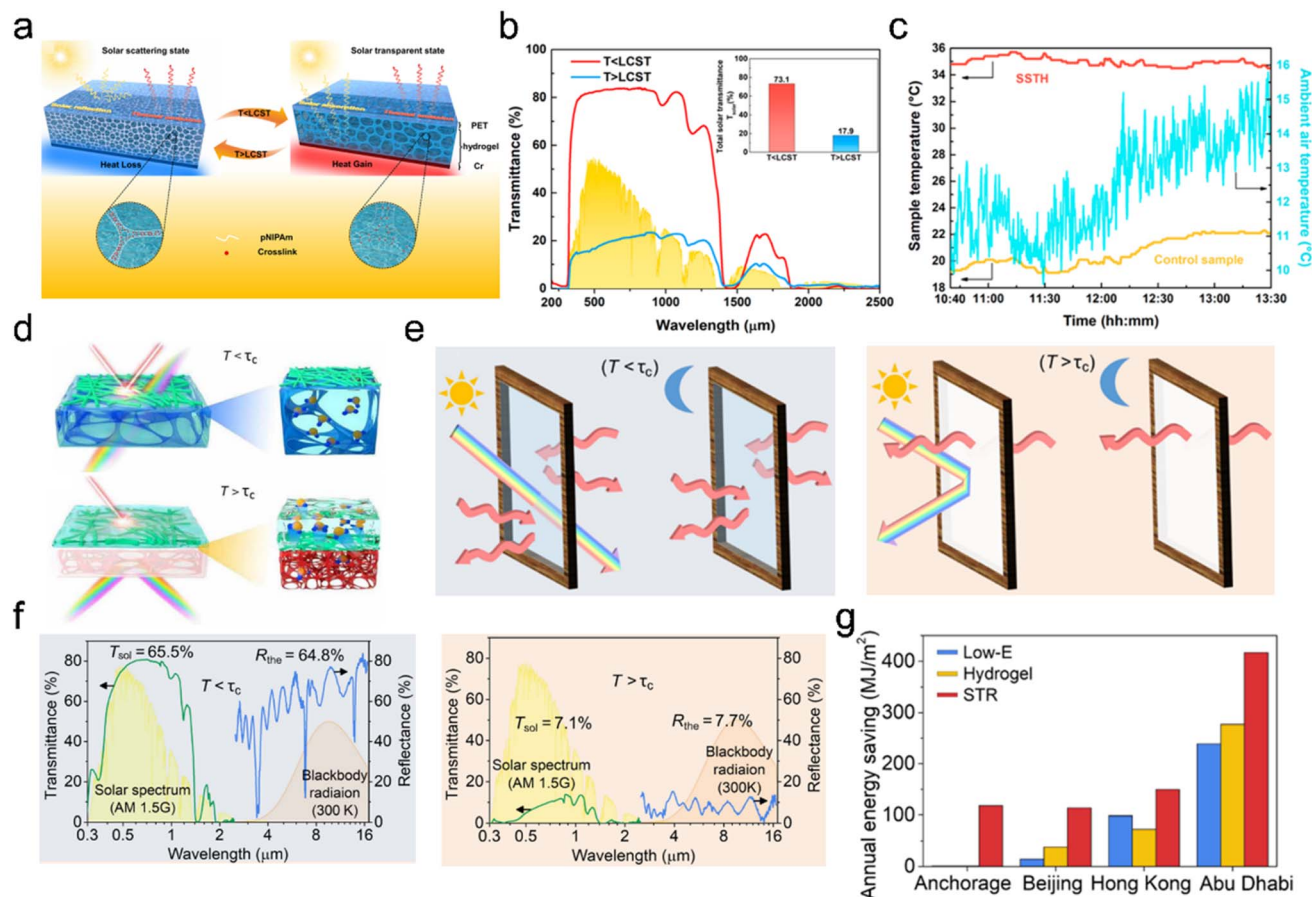


Fig. 13 The adaptive cooling materials based on pNIPAm hydrogels. (a) Schematic of the switching of solar transmittance based on pNIPAm hydrogels. (b) The regulation of solar transmittance with pNIPAm hydrogels. (c) The temperature variation of adaptive cooling films with pNIPAm hydrogels. (d) Schematic of the working mechanism of adaptive cooling films with pNIPAm hydrogels. (e) Schematic of the regulation of solar and mid-infrared radiation for pNIPAm-based adaptive cooling films. (f) The spectral profiles of pNIPAm-based adaptive cooling films under high and low temperature conditions. (g) The annual energy saving of pNIPAm-based adaptive cooling films in different areas. (a–c) Reproduced with permission from ref. 147 Copyright 2021 American Chemical Society. (d–g) Reproduced with permission from ref. 13 Copyright 2022 AAAS.

even in smart windows.<sup>148,149</sup> Moreover, their inferior mechanical properties can lead to shrinkage and water loss or absorption in hydrogels, further impacting their performance.

## 5 Applications of cooling technology

The significant advancements in RSC technology have led to extensive research efforts focused on its practical applications in buildings.<sup>48,151–153</sup> Cooling materials can be applied in two ways: through direct integration with the building envelope or indirect integration with cooling systems. In direct applications, cooling materials can be applied to the building envelope. By incorporating RSC materials into the building surface, heat is effectively dissipated to the sky based on passive cooling. This approach offers a simple and cost-effective solution to improve thermal comfort and reduce energy consumption.

Indirect integration involves using cooling materials to develop cooling devices and systems that can be integrated with the existing air-conditioning systems for building cooling purposes. These cooling devices leverage the radiative properties of the materials to enhance heat dissipation. By coupling

RSC technology with conventional cooling systems, energy efficiency can be improved, thus reducing the reliance on traditional cooling methods and decreasing overall energy consumption.

### 5.1 Building envelope cooling

As discussed above, the continuous operation of radiative cooling can lead to increased heating energy consumption during winter in mid-latitude regions, compromising its cooling effectiveness in summer. Despite the advancements in self-adaptive cooling materials, their practical application is hindered by high cost, complex processing and limited stability. Therefore, the direct application of cooling materials on building envelopes remains a topic of debate when considering building energy efficiency and human comfort, especially in mid-latitude regions where a significant portion of the population resides.

However, it is worth noting that RSC technology has demonstrated significant potential for specific building applications, *e.g.*, temporary houses,<sup>154</sup> granaries<sup>155</sup> and base station. In these specialized settings, the unique requirements and

constraints make the implementation of RSC technology more feasible and beneficial. For instance, temporary houses often require quick and cost-effective cooling solutions, making RSC technology an attractive option. Similarly, granaries and base stations may benefit from the passive cooling capabilities of RSC technology to maintain optimal storage conditions or protect sensitive equipment. The cooling capacity from RSC materials can be quickly transferred to indoors, which can block the strong solar heating and maintain sub-ambient temperature for temporary buildings (Fig. 14a and b). For instance, Zhang *et al.*<sup>154</sup> investigated the working performance of cooling paints in different buildings and they found that pre-fabricated container houses can achieve a sub-ambient temperature drop of 10.6 °C and the roof temperature difference can reach ~33.1 °C, compared with the control container houses. With these benefits, the container houses can achieve an indoor temperature drop of ~11.4 °C, resulting in an energy saving of 38.8%.

In addition, cooling materials also present great application potential in some special envelopes with internal heat generation, *e.g.*, granary, oil tank, chemical storage tank and base station. For grain storage, it is highly essential to maintain low temperature to inhibit heat generation in crops, which can otherwise lead to germination or metamorphism (Fig. 14d). Moreover, edible oil will be quickly deteriorated at high temperatures under strong solar radiation and RSC technology can help address this issue. For instance, Cai *et al.* developed self-cleaning sub-ambient cooling paints for concrete grain granaries and edible oil storage tanks.<sup>155</sup> With the promising cooling paints, the grain granary and edible oil storage tank presented temperature drops of ~37 °C and 33 °C, respectively, resulting in an interior temperature drop of 10 °C and 4 °C for wheat pile and edible oil. Similarly, cooling coatings can also significantly reduce the temperature of chemical storage tanks, which can alleviate the evaporative loss of chemicals. Tso's

group<sup>159</sup> developed a polymeric cooling coating for chemical storage tanks, which can enable saving of chemicals up to ~81.4% and 54.1%, compared with that of raw containers and containers with commercial paints. For base stations, the working of electronic equipment produces abundant heat, resulting in rapid temperature rise and the corresponding performance degradation (Fig. 14e). In the recent study by Cai *et al.*,<sup>157</sup> the performance of cooling paints for telecommunication base stations was investigated. The researchers found that the application of cooling paints on base stations resulted in a significant temperature drop of 24.2 °C. This temperature drop demonstrates the cooling effectiveness of the paints in the context of telecommunication base stations. Additionally, over a working period of 290 days, the implementation of cooling paints resulted in a substantial electricity saving of 1038.4 kW h. These findings highlight the energy-saving potential of cooling paints in the context of telecommunication base stations, offering both thermal management benefits and reduced energy consumption.

For ordinary buildings, the direct applications of RSC technology has shown promising results in terms of significant energy savings for cooling systems, as revealed by some modeling studies.<sup>48,151,160</sup> In addition to energy savings, the reports have also discussed the economics and environmental impact of RCS technology applications, all of which demonstrate its great potential in buildings.<sup>48,151</sup> Moreover, researchers have made notable efforts to validate the energy-saving benefits of RSC technology through modeling and real-world experiments. In 2019, Fang *et al.*<sup>44</sup> employed a promising metamaterial-based cooling roof on model buildings and developed a model with an improved roof thermal transfer value. This approach revealed significant energy savings ranging from 113.0 to 143.9 kW h/(m<sup>2</sup> per years). Similarly, Yan's group<sup>152,161</sup> also investigated the performance of

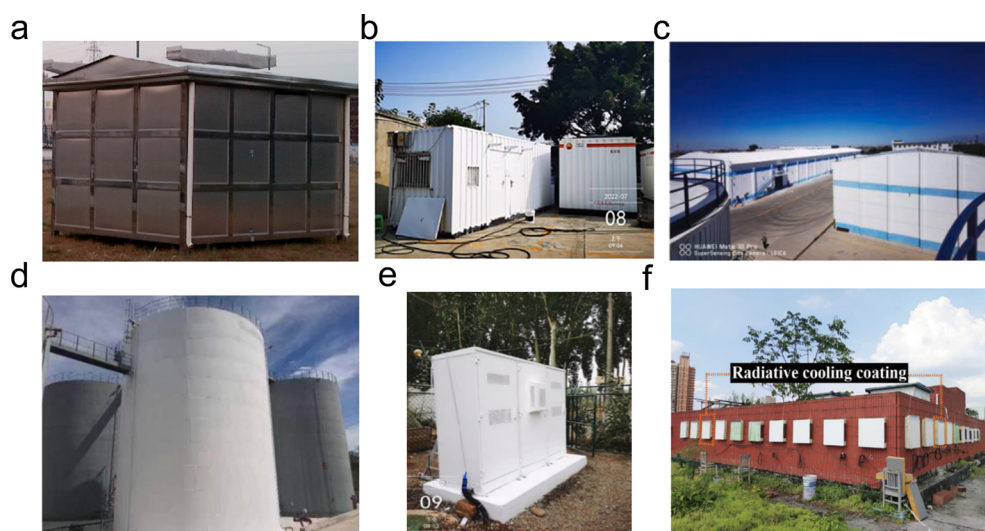


**Fig. 14** The direct applications of RSC in buildings. (a–c) The photograph of RSC applications in temporary houses. (d) Photograph of a granary with cooling paints. (e) Photograph of a base station with cooling paints. (f) The photograph of buildings with cooling paints on the façade side. (a) Reproduced with permission from ref. 156 Copyright 2022 Elsevier. (b) Reproduced with permission from ref. 154 Copyright 2022 Elsevier. (c and d) Reproduced with permission from ref. 155 Copyright 2023 Elsevier. (e) Reproduced with permission from ref. 157 Copyright 2023 Elsevier. (f) Reproduced with permission from ref. 158 Copyright 2023 Elsevier.

spectrum-selective RSC materials on model buildings and further developed the radiative cooling model, which can integrate with the commercial building consumption simulation software, *e.g.*, DeST tool. The modeling results showcased the energy-saving potential of RSC technology, with savings ranging from 14% to 42% for single-storey commercial buildings in six different locations worldwide. In addition, Lei *et al.*<sup>158</sup> evaluated the performance of cooling coatings under various installation orientations. They found that the cooling performance of coatings on a horizontal surface significantly decreased after four months of operation due to dust accumulation (Fig. 14f). This highlights the importance of regular maintenance and cleaning to ensure the continued effectiveness of cooling coatings.

While the direct applications of cooling materials may lead to over-cooling during nighttime and winter, it is evident that this approach still holds significant energy-saving potential, particularly in the face of the increasingly severe global warming. Despite the challenges associated with over-cooling, there are numerous promising application scenarios for RSC technology. For instance, RSC technology can find valuable applications in emergency shelters and the covered bridges for

airport terminals and subway stations. These environments often require abundant cooling capacity to counteract the intense thermal disturbances in hot climates. RSC technology can provide an efficient and sustainable cooling solution in such scenarios.

To address the issue of over-cooling, the combination of cooling materials with phase change materials (PCMs) has shown promise. PCMs can absorb excess cooling during nighttime or winter and release it when needed, helping to balance the cooling effect. This combination approach can broaden the application range of RSC technology and mitigate the challenges associated with over-cooling.<sup>162–165</sup> Furthermore, advancements in self-adaptive cooling materials hold the potential for significant cooling energy savings in buildings.

## 5.2 Building device cooling

To facilitate the practical implementation of the RSC technology, the development of various cooling devices for building integration and cooling supply is crucial.<sup>26</sup> Researchers have made notable advancements in this area, designing innovative cooling devices with impressive capabilities.

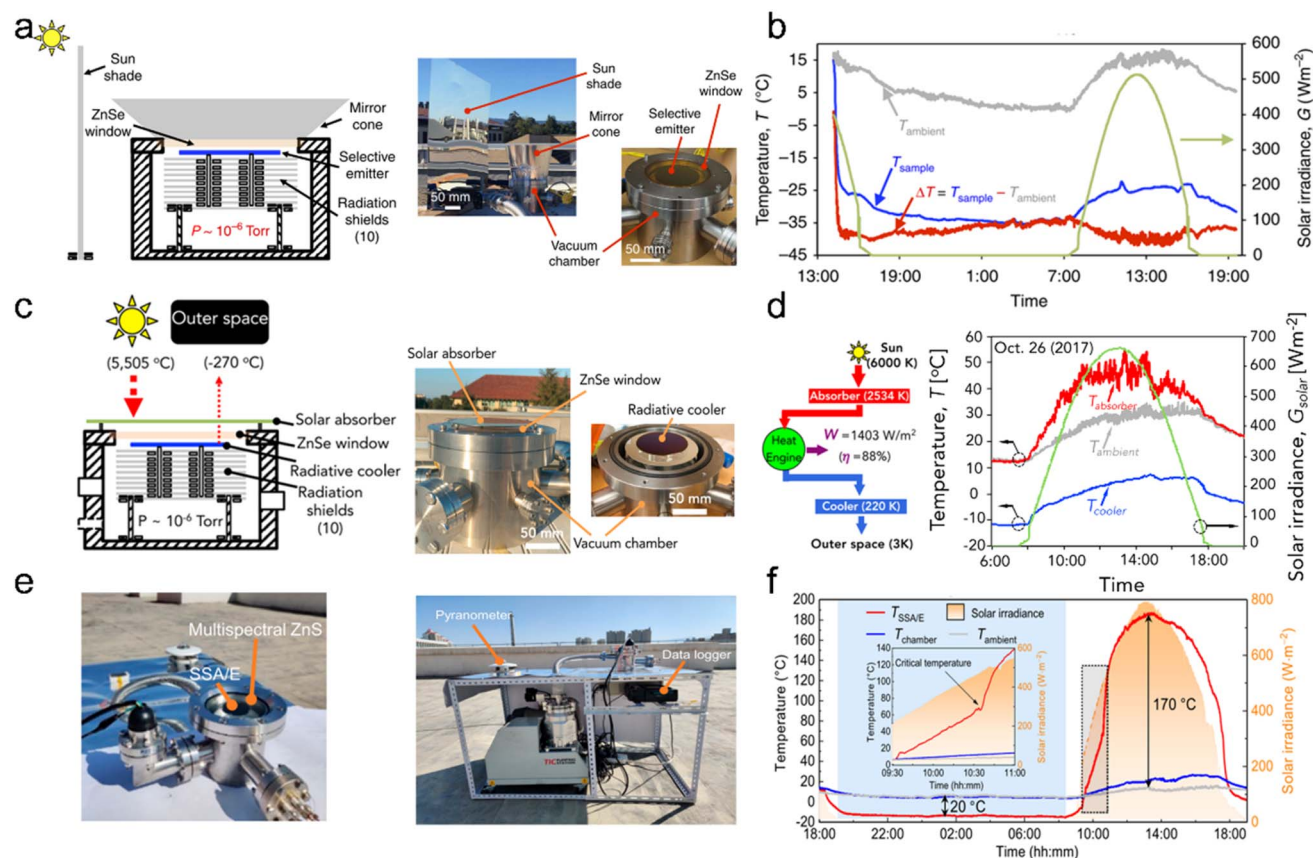


Fig. 15 Radiative cooling devices with vacuum chambers. (a) Schematic and photograph of cooling devices with vacuum chambers. (b) The cooling performance of the devices with vacuum chambers. (c) Schematic and photograph of vacuum-chamber devices with solar filtering. (d) The theoretical limitations and cooling performance of the devices with solar filtering. (e) The photograph of vacuum-chamber devices with self-adaptive photonic films. (f) The cooling performance of vacuum-chamber devices with self-adaptive photonic films. (a and b) Reproduced with permission from ref. 26 Copyright 2016 Springer Nature. (c and d) Reproduced with permission from ref. 166 Copyright 2019 Elsevier. (e and f) Reproduced with permission from ref. 142 Copyright 2022 AAAS.



**5.2.1 Vacuum-chamber cooling devices.** In 2016, Chen *et al.* designed a remarkable cooling device based on a vacuum chamber and an infrared-transmission window (Fig. 15a).<sup>26</sup> This device, with selective emissivity and extremely low thermal conductivity, achieved a maximum sub-ambient temperature drop of 42 °C and an average temperature drop of 37 °C when combined with the external sunshade. This demonstrated the significant application potential of RSC technology in cryo-preservation of food and medicine (Fig. 15b). However, the reliance on external sunshades limited its practical application. To overcome this limitation, the group further utilized infrared-transmission germanium semiconductor materials to eliminate solar heating for the underlying radiative cooler (Fig. 15c).<sup>166</sup> This improved device simultaneously harvested solar heating and provided radiative cooling, resulting in an above-ambient temperature rise of 24 °C and a sub-ambient temperature drop of 29 °C (Fig. 15d). This promising design substantially enhanced the application potential of the device. However, harvesting the heat from the upper solar heating layer remained challenging due to the stringent requirements of high infrared

transmittance. Furthermore, Pei's group<sup>142</sup> employed a multi-layer VO<sub>2</sub> photonic structure for self-adaptive conversion of mid-infrared emissivity. This design enabled an above-ambient temperature rise of 170 °C during the daytime and a sub-ambient temperature drop of 20 °C during the nighttime (Fig. 15e and f). Moreover, the integrated design of solar heating and radiative cooling facilitated the provision of both heating and cooling capacity. Nevertheless, the use of a vacuum chamber posed limitations of their practical applications in buildings.

**5.2.2 Waveguide cooling devices.** In addition to the advisements in cooling device design, there are also promising designs of cooling devices based on waveguide structures. For instance, Zhou *et al.*<sup>167</sup> developed cooling devices with facade emitters and two spectrally selective mirrors, resulting in significantly enhanced radiative cooling performance (Fig. 16a–c). These double-sided cooling devices achieved a sub-ambient temperature drop of ~14 °C and a cooling power density of over 270 W m<sup>-2</sup>, which were notably higher than those of single-sided devices (Fig. 16d–f). This improvement demonstrates the

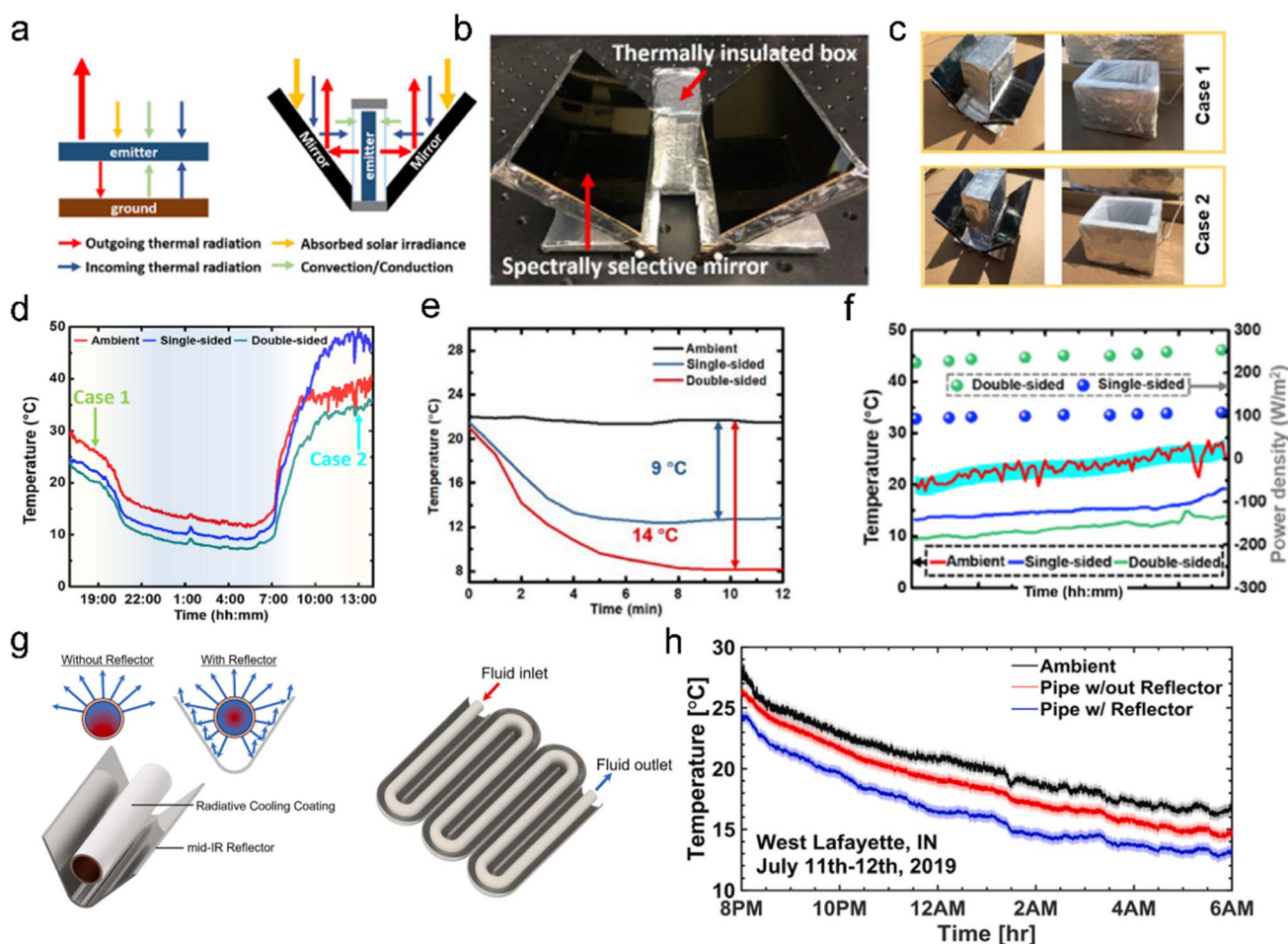


**Fig. 16** The promising radiative cooling devices. (a–c) Schematic and photograph of cooling devices with a facade emitter and two spectrally selective mirrors. (d) The cooling performance of the devices with a facade emitter in two cases. (e) The cooling performance of the devices with single-sided and double-sided mirrors. (f) The temperature drop and cooling power of the two devices with single or double mirrors. (g and h) The concentrated radiative cooling devices and the corresponding cooling performance. (a–f) Reproduced with permission from ref. 167 Copyright 2021 Elsevier. (g and h) Reproduced with permission from ref. 168 Copyright 2022 Elsevier.

potential for more efficient and effective cooling using spectrally selective mirrors. Moreover, Ruan's group<sup>168</sup> recently introduced the concept of concentrated radiative cooling by integrating a cooling pipeline with a mid-infrared reflective trough (Fig. 16g). This approach enables strong infrared emission from the entire pipeline surface. As a result, the developed devices achieve substantially improved temperature drops, approximately twice as much as those without the reflective trough (Fig. 16h). Importantly, these devices can be easily integrated with air-conditioning systems, offering a practical solution for implementing RSC technology.

In urban environments, commonly used radiative cooling devices can experience reduced cooling performance due to partial obstruction of the access to the sky by nearby buildings (Fig. 17a). For instance, the same radiative coolers on the roof of high-rise buildings can achieve a significant cooling temperature drop of 11 °C, but the values decrease to ~7.2 °C and 2.5 °C in the middle and bottom of buildings (Fig. 17b).<sup>169</sup> To

overcome this challenge, Zhou *et al.* devised promising cooling devices with a tapered waveguide structure, which effectively suppresses solar input and reflects mid-infrared light from radiative coolers (Fig. 17c and d).<sup>169</sup> With this innovative design, the devices can achieve similar cooling performance across different urban environments, which is highly favorable for the practical applications of RSC technology (Fig. 17e). Furthermore, these devices can be easily integrated onto the roof of buildings, providing efficient cooling capacity for an indoor environment. However, it is important to address several critical issues to ensure the successful implementation of these devices. Factors such as cost, weather resistance, and the accumulation of water and ash should be carefully considered. Cost-effective manufacturing processes and materials should be explored to make these cooling devices accessible and affordable. Additionally, the devices should be designed to withstand various weather conditions and resist degradation over time. Proper measures should also be implemented to prevent the

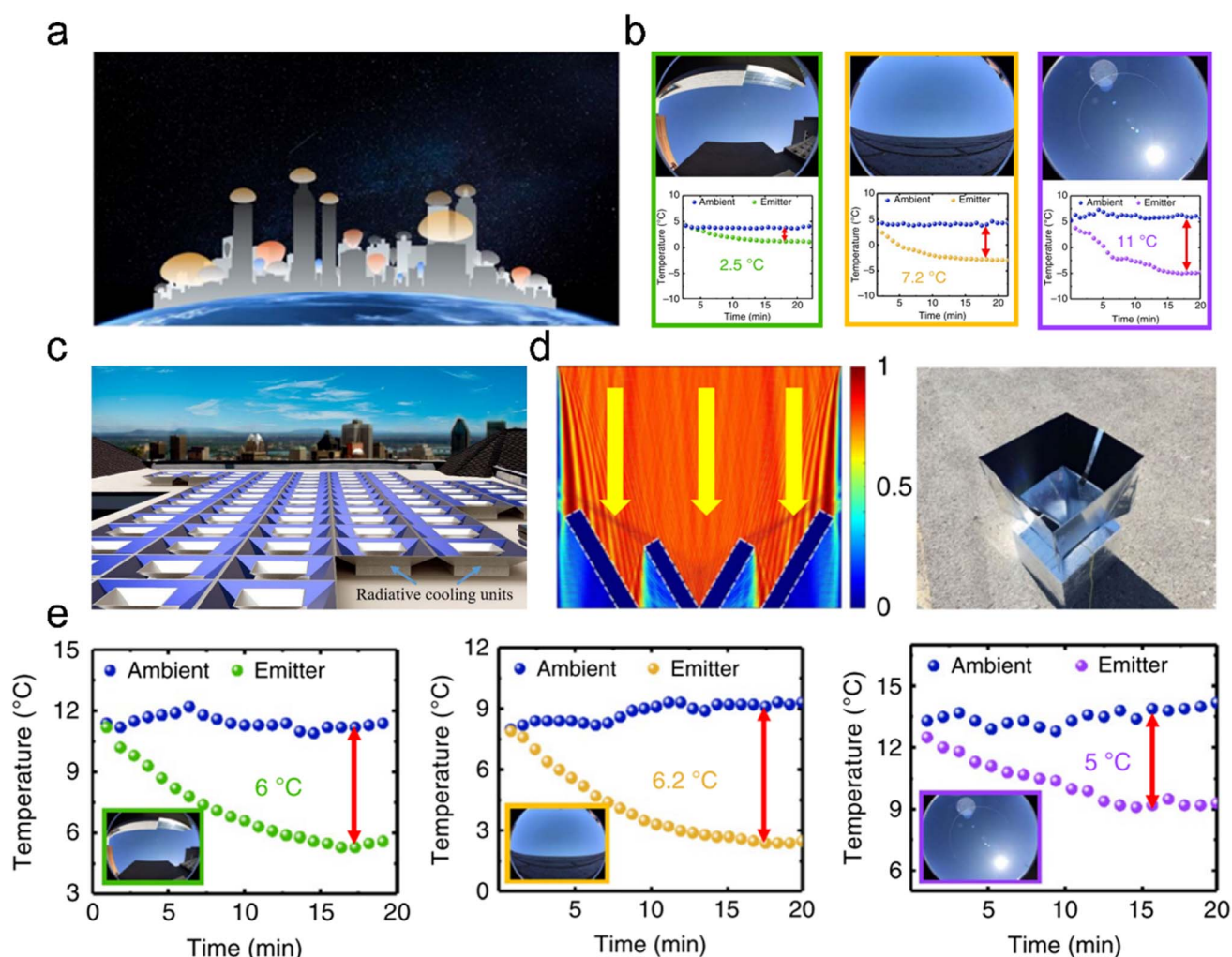


Fig. 17 Promising radiative cooling devices with a tapered waveguide structure. (a) Schematic of infrared emission intensity of buildings with different heights in a city. (b) The radiative cooling performance in city buildings with different heights. (c) Schematic of cooling devices with a tapered waveguide structure. (d) The photograph of cooling devices and the modelled beam propagation distribution in the device. (e) The cooling performance of the developed devices in the city buildings with different heights. (a–e) Reproduced with permission from ref. 169 Copyright 2019 Springer Nature.



accumulation of water and ash, which can hinder the performance of the cooling devices.

To the best of our knowledge, limited research has focused on addressing the cost implications for practical applications. Given the moderate cooling power ( $\sim 100 \text{ W m}^{-2}$ ) of RSC technology,<sup>170–173</sup> there is a concern that high processing and material costs could undermine its advantages over the conventional cooling methods. Therefore, it is crucial to investigate cost-effective manufacturing processes and materials to enhance the economic viability of RSC technology. Additionally, more research efforts should be directed towards examining the weather resistance of RSC devices to ensure their continuous and stable operation under various environmental conditions. Factors such as temperature variations, humidity, sunlight exposure, and precipitation should be considered to enhance the durability and performance of RSC devices. When developing vacuum-chamber based devices for building applications, careful considerations should be given to the design of heat conduction and cooling capacity. However, it is important

to note that introducing heat-conduction devices may potentially compromise the achieved cooling performance in real-world environments. Therefore, striking a balance between heat conduction and cooling capacity is a challenge that needs to be addressed to optimize the performance of RSC devices.

### 5.3 Building air-conditioning cooling

To leverage the cooling potential of outer space for buildings while avoiding over-cooling in a cold environment, it is advantageous to develop innovative cooling designs that can be integrated into buildings. In this section, we summarize the recent advances in building air-conditioning cooling from the two sub-sections: radiative water cooling and radiative air cooling.

**5.3.1 Radiative water cooling.** In the initial stage, Fan's group<sup>3</sup> developed prototype cooling panels comprising radiative cooling films, copper pipes and insulation materials. These panels effectively cooled the fluid below ambient temperature

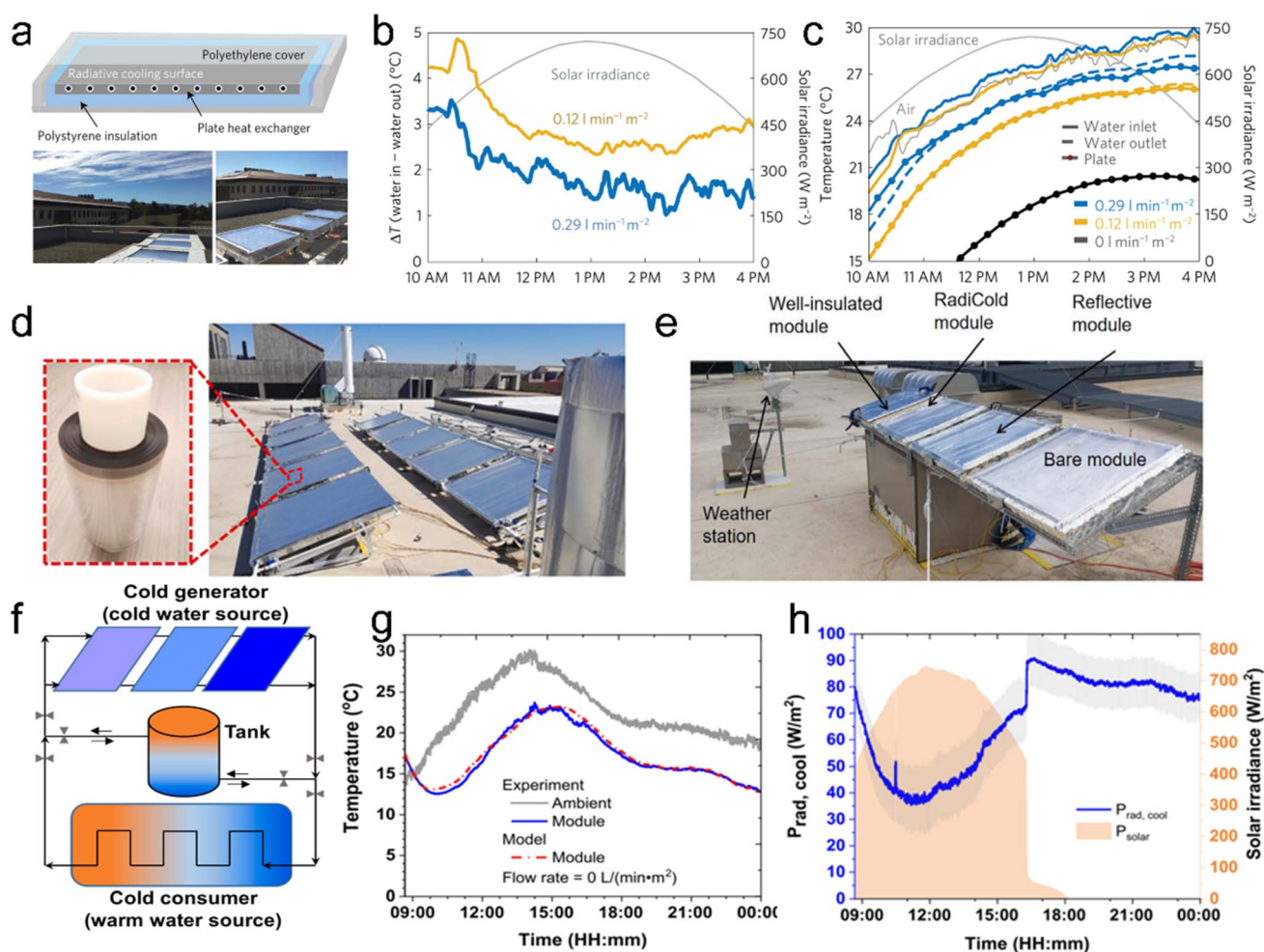


**Fig. 18** The promising cooling systems for building applications. (a) Schematic and photograph of cooling modules. (b) The temperature drop of cooling modules with different flow velocities. (c) The actual cooling performance of the developed cooling system. (d and e) The photographs of cooling systems with great cooling performance and application potential. (f) Schematic of radiative cooling systems with energy storage tanks. (g) The theoretical and practical cooling performance of the cooling module. (g) The cooling power of the systems in daytime and nighttime. (a–c) Reproduced with permission from ref. 3 Copyright 2017 Springer Nature. (d and f–h) Reproduced with permission from ref. 39 Copyright 2019 Elsevier. (e) Reproduced with permission from ref. 38 Copyright 2019 Elsevier.



(Fig. 18a). With a three-day testing, the panels could cool water fluid by 5 °C below the ambient temperature, corresponding to a cooling power of 70 W m<sup>-2</sup> (Fig. 18b and c). Modeling results revealed that integrating these cooling panels on the condenser side of an air-conditioning system could lead to electricity savings of ~21% for a two-storey building.

Building upon this work, Zhao *et al.*<sup>38</sup> further developed cooling systems based on RSC films, straight pipelines, and insulation materials (Fig. 18d and e). These promising cooling systems achieved a remarkable cooling effect, reducing the water temperature by 10.6 °C below the ambient temperature during daytime hours under stationary conditions. The researchers also constructed a kilowatt-scale cooling system, capable of delivering a maximum cooling power of 1296 W at night with the flow rate of 26.5 L (h<sup>-1</sup> m<sup>-2</sup>). Modeling results demonstrated that this cooling system had a potential saving 32–45% of electricity consumption for buildings during

summer. Furthermore, the group demonstrated that the kilowatt-scale cooling system could sustain continuous cooling performance and enhance building energy efficiency by incorporating energy-storage devices (Fig. 18f and g).<sup>39</sup> This integration of energy storage devices further improved the overall energy-saving capabilities of the cooling system.

**5.3.2 Radiative air cooling.** In addition to the advancements in cooling water systems, there are some promising integration methods with buildings that offer enhanced cooling capacity and energy savings. One approach is to integrate radiative cooling systems with the attic of buildings (Fig. 19a).<sup>174</sup> Zhao *et al.* developed an RSC module and corresponding system for a single-family house with an attic (Fig. 19c–e).<sup>174</sup> This system effectively reduces the attic temperature by 15.5–21.0 °C, compared to a shingle roof during summer. As a result, the developed system enables annual cooling energy savings of 26.5–76.1% for different roof structures in Phoenix (Fig. 19f).

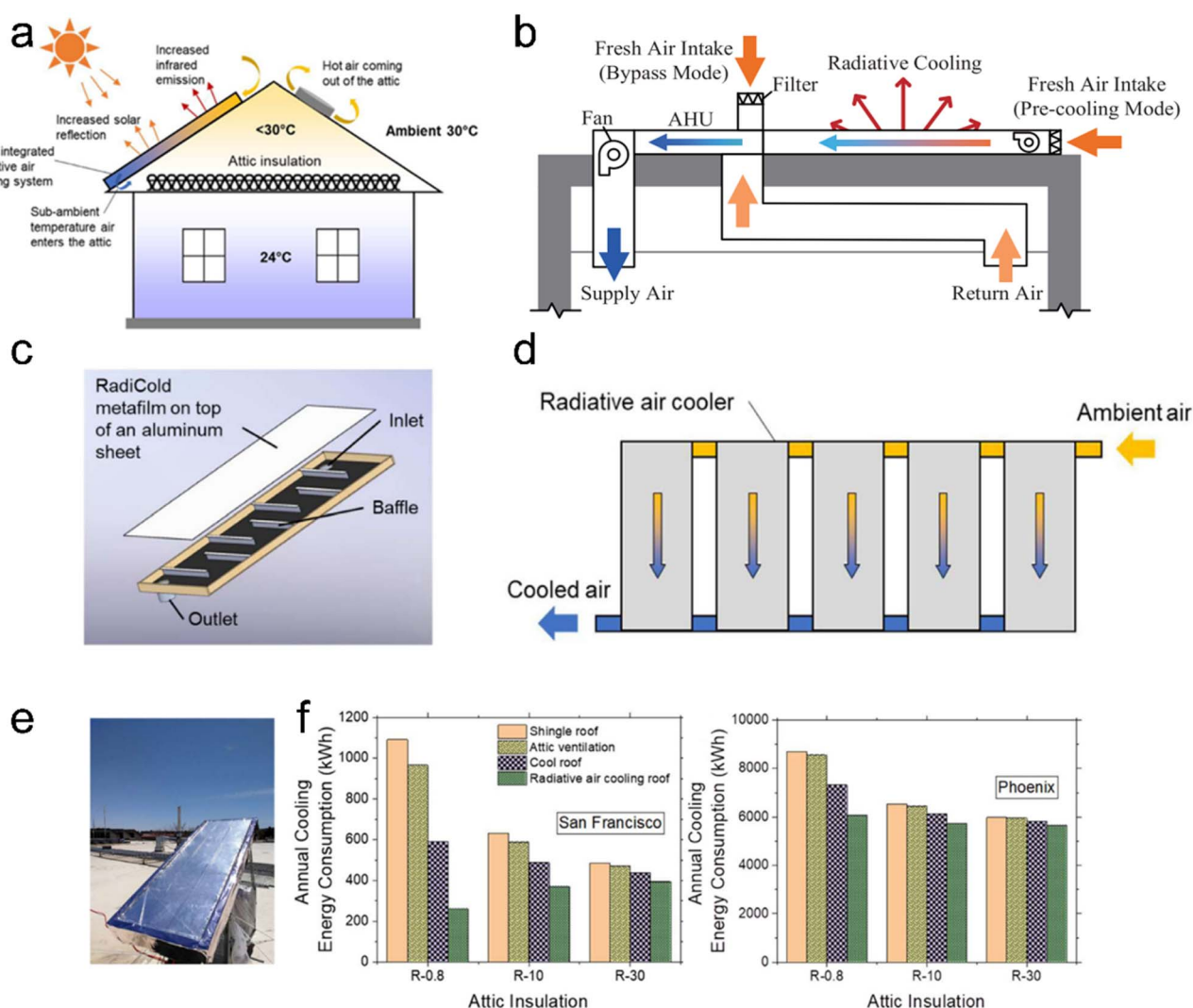


**Fig. 19** The other promising designs of cooling systems. (a) Schematic of the integration of the radiative cooling module with the attic of buildings. (b) Schematic of the pre-cooling of cooling systems based on radiative cooling. (c and d) Schematic of the radiative air cooling module and the corresponding integrated design. (e) The photograph of the radiative air cooling module. (f) The building energy saving with different structures in San Francisco and Phoenix. (a and c–f) Reproduced with permission from ref. 174 Copyright 2019 Elsevier. (b) Reproduced with permission from ref. 175 Copyright 2022 Springer.

Moreover, radiative cooling systems can also be employed to provide the pre-cooling of supply air for air-conditioning systems (Fig. 19b). Zhang *et al.* proposed cooling systems for a two-floor single-family house with low cooling load and a high-ratio roof area, which are favorable conditions for implementing the RSC technology.<sup>160</sup> Air pre-cooling using these systems can achieve annual cooling energy savings of 26–46% for the modeled locations, with the payback of approximately 4.8–8 years. Furthermore, Zhao *et al.* developed a novel radiative cooling-assisted thermoelectric cooling system, which aims to reduce the cooling energy consumption of two-storey residential buildings.<sup>176</sup> By incorporating the RSC sub-system, this hybrid cooling system achieves an enhanced annual coefficient of performance (COP) of 1.87. Importantly, the annual cooling performance and energy savings of building-integrated cooling systems can harness excess cooling capacity during the nighttime, enhancing overall system efficiency.

In addition to standalone applications, there is a growing interest in integrating radiative cooling and solar heating into a single system to provide simultaneous cooling and heating capacities for buildings. Pei's group has made significant contributions to the development of integrated systems for radiative cooling and solar heating.<sup>177–182</sup> They have designed various hybrid modules and systems that supply hot water during the daytime and cold water during the nighttime. However, these integrated systems often face challenges in providing sufficient cooling capacity for buildings during the daytime, and the high infrared emissivity of radiative cooling components can result in substantial heat loss during solar harvesting. To address these challenges, some reports proposed innovative combinations of radiative cooling and solar harvesting tailored to specific building structures. For instance, Hu's group proposed a novel integration strategy that utilizes a solar chimney on the sunny side and a radiative cooling cavity on the backlit side.<sup>183</sup> This design enables a maximum temperature reduction of 2 °C compared to the ambient temperature and significantly enhances ventilation rates. Furthermore, a hybrid strategy can be employed to integrate photovoltaics and radiative cooling modules, providing both electrical power generation and cooling capacities.

While the development of radiative cooling systems holds promise for building applications, it also introduces complexities and costs that could limit its implementation potential. Typically, radiative coolers achieve moderate cooling power ( $\sim 100 \text{ W m}^{-2}$ ) and daytime temperature reduction of around 5 °C, which may hinder their widespread adoption in buildings.<sup>61,184–187</sup> Therefore, it is critical to dedicate more research efforts towards developing low-cost and easily deployable cooling systems with enhanced cooling performance. In this regard, the concentrated radiative cooling modules developed by Ruan's group present substantial potential for application in buildings, thanks to their significantly enhanced cooling performance and streamlined design.<sup>168</sup>

## 6 Summary and outlook

With regard to the rapid progress of RSC technology in the past decade, it's time to thoroughly summarize the recent advances of

RSC materials and their promising application in building energy saving. This review presented the basic requirements with large-scale and low-cost cooling materials including cooling films and cooling paints in building applications. Subsequently, we systematically discussed the functional requirements of various RSC materials in building application. For aesthetic considerations, buildings generally require multiple colors, which motivate the research of colorful cooling materials for actual applications. Moreover, durability is another critical index for the actual applications of cooling materials in buildings and the recent efforts in developing durable cooling materials are highlighted, especially for their great potential in countering harsh working environments. Moving forward, the direct applications of cooling materials will increase the heating energy consumption of buildings in winter, which aroused the development of bifunctional materials and adaptive cooling materials. The recent research efforts and advances of these two promising materials are outlined to reveal their application potential and the existing challenges in actual applications.

In addition, this review further summarized the recent efforts in advancing the building applications of cooling materials and discussed in detail the different ways of combining them with buildings, mainly including direct building cooling, building cooling devices and building cooling systems. On the whole, the direct building cooling method has great application potential in reducing building energy consumption due to the large cooling areas of cooling materials on building envelopes. However, the increased energy consumption in winter still places great restrictions on their actual applications. In addition, the promising designs of cooling devices and systems were further highlighted for their great cooling supply and storage for building applications. Despite the great progress, there still remain some open challenges for the actual applications of RSC technology in buildings. We proceed to present a brief discussion on the critical issues and offer our insights into the corresponding research directions (Fig. 20).

### 6.1 Multifunctional integration materials

In practical architectural applications, it is often necessary to integrate several functions at the same time, such as the need to maintain color and durability at the same time. Generally, the commonly used pigments present strong solar absorption, resulting in the excessive solar heating of cooling materials and inferior cooling performance.<sup>14,188</sup> The emerging quantum dot materials can not only deliver great cooling performance, but also present multiple colors for building applications. However, quantum dot materials generally have some stability issues in harsh environments with water, oxygen and high-energy ultraviolet radiation,<sup>189–191</sup> which will destroy the colloid structure and accelerate the degradation rate, blocking their actual applications in buildings. On the other hand, the harsh environment also has a great impact on the durability of white cooling materials, especially under ultraviolet radiation. Therefore, future research should invest more experience in the development of radiative cooling building materials with multifunctional integration.

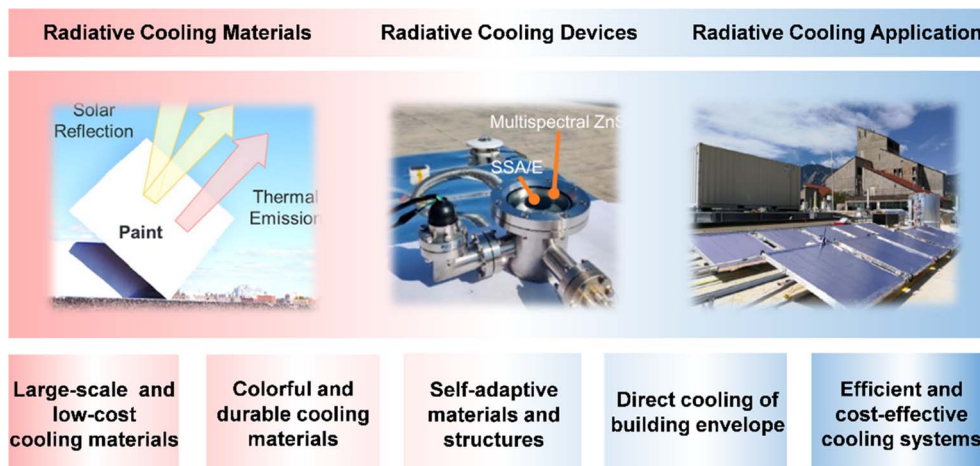


Fig. 20 Summary of the challenges and research directions for the actual applications of RSC technology in buildings.

### 6.2 Cooling power for building application in hot summers

The direct application of radiative cooling materials in building envelopes can significantly reduce the cooling energy consumption of buildings, especially with the continuous increase of global warming and extreme weather. However, a radiative cooling power of  $100 \text{ W m}^{-2}$  is not sufficient to withstand the high temperature environment, especially in hot areas. Notably, the cooling power inefficiency issues can be addressed by the introduction of phase change materials or evaporative cooling materials, which can enable remarkable building energy saving and broaden the application range of RSC technology. Therefore, research on radiative cooling technology coupled with other passive cooling technologies needs to be further explored to achieve cooling gains and greater energy efficiency gains for buildings.

### 6.3 Over-cooling for building application in cold winters

It is well established that the direct applications of cooling materials on building envelopes may significantly increase the building energy consumption in the winter of mid-latitude regions. With regard to this issue, more research efforts have been made to develop self-adaptive materials, which can present strong infrared emission in a hot environment and low infrared emission in a cold environment. Although various self-adaptive materials (e.g.,  $\text{VO}_2$  and pNIPAM hydrogels) have been developed in the past few years,<sup>31,147,192</sup> their actual applications may be still blocked by the complicated processing, high cost and poor stability. More research is encouraged to design facile and cost-effective self-adaptive materials/structures for building applications. The recent work by Long's group developed self-adaptive coolers based on kirigami structures and pNIPAM hydrogel coated with silver nanowires.<sup>148</sup> The self-adaptive regulation of solar transmittance and mid-infrared emissivity can be fulfilled by thermochromic hydrogels and stretching-induced shape morphing structures, respectively. The low cost and facile structure enable their great application potential in glass curtain walls and windows of buildings.

### 6.4 Efficient and cost-effective cooling devices and systems

Cooling devices and systems can control the input and output of cooling capacity for buildings, which can address the over-cooling effect of RSC technology. Some promising cooling devices and systems have been developed in the past few years.<sup>167–169</sup> Although some cooling devices can achieve record cooling performance under a vacuum state, it is hard to collect the cooling capacity produced by the vacuum-chamber devices. In contrast, the concentrated radiative cooling modules hold great application potential in buildings due to the enhanced cooling performance and facile integration with cooling systems.<sup>168</sup> It can be expected that RSC technology can enable great cooling energy saving in buildings with the great advance of low-cost and facile cooling devices and systems.

## Data availability

No primary research results, software or code have been included and no new data were generated or analysed as part of this review.

## Author contributions

K. Huang: formal analysis, visualization, writing – original draft, data curation. Z. Huang: writing – review & editing. Y. Du: writing – review & editing, investigation. Y. Liang: writing – review & editing. J. Liu: conceptualization, supervision, writing – review & editing. J. Yan: supervision, writing – review & editing.

## Conflicts of interest

The authors declare no competing financial interests.

## Acknowledgements

The authors would like to especially acknowledge the National Key R&D Program of China (No. 2023YFE0203900).



## References

- 1 R. M. DuChanois, N. J. Cooper, B. Lee, S. K. Patel, L. Mazurowski, T. E. Graedel and M. Elimelech, *Nat. Water*, 2023, **1**, 37–46.
- 2 R. Dai, H. Zhou, T. Wang, Z. Qiu, L. Long, S. Lin, C. Y. Tang and Z. Wang, *Nat. Water*, 2023, **1**, 281–290.
- 3 E. A. Goldstein, A. P. Raman and S. Fan, *Nat. Energy*, 2017, **2**, 17143.
- 4 X. Wang, Z. Lin, J. Gao, Z. Xu, X. Li, N. Xu, J. Li, Y. Song, H. Fu, W. Zhao, S. Wang, B. Zhu, R. Wang and J. Zhu, *Nat. Water*, 2023, **1**, 391–398.
- 5 J. Liu, Z. Zhou, D. Zhang, S. Jiao, J. Zhang, F. Gao, J. Ling, W. Feng and J. Zuo, *Energy Convers. Manag.*, 2020, **205**, 112395.
- 6 R. A. Kishore, A. Nozariasbmarz, B. Poudel, M. Sanghadasa and S. Priya, *Nat. Commun.*, 2019, **10**, 1765.
- 7 W. He, G. Zhang, X. Zhang, J. Ji, G. Li and X. Zhao, *Appl. Energy*, 2015, **143**, 1–25.
- 8 W. Chen, X. Shi, J. Zou and Z. Chen, *Mater. Sci. Eng. R*, 2022, **151**, 100700.
- 9 H. Cui, Q. Zhang, Y. Bo, P. Bai, M. Wang, C. Zhang, X. Qian and R. Ma, *Joule*, 2022, **6**, 258–268.
- 10 J. Shi, D. Han, Z. Li, L. Yang, S. G. Lu, Z. Zhong, J. Chen, Q. M. Zhang and X. Qian, *Joule*, 2019, **3**, 1200–1225.
- 11 S. Qian, D. Catalini, J. Muehlbauer, B. Liu, H. Mevada, H. Hou, Y. Hwang, R. Radermacher and I. Takeuchi, *Science*, 2023, **380**, 722–727.
- 12 R. Wang, S. Fang, Y. Xiao, E. Gao, N. Jiang, Y. Li, L. Mou, Y. Shen, W. Zhao, S. Li, A. F. Fonseca, D. S. Galvão, M. Chen, W. He, K. Yu, H. Lu, X. Wang, D. Qian, A. E. Aliev, N. Li, C. S. Haines, Z. Liu, J. Mu, Z. Wang, S. Yin, M. D. Lima, B. An, X. Zhou, Z. Liu and R. H. Baughman, *Science*, 2019, **366**, 216–221.
- 13 C. Lin, J. Hur, C. Y. H. Chao, G. Liu, S. Yao, W. Li and B. Huang, *Sci. Adv.*, 2022, **8**, eabn7359.
- 14 Y. Chen, J. Mandal, W. Li, A. Smith-Washington, C. C. Tsai, W. Huang, S. Shrestha, N. Yu, R. P. S. Han, A. Cao and Y. Yang, *Sci. Adv.*, 2020, **6**, eaaz5413.
- 15 P. C. Hsu, A. Y. Song, P. B. Catrysse, C. Liu, Y. Peng, J. Xie, S. Fan and Y. Cui, *Science*, 2016, **353**, 1019–1023.
- 16 P. Hsu, C. Liu, A. Y. Song, Z. Zhang, Y. Peng, J. Xie, K. Liu, C. Wu, P. B. Catrysse, L. Cai, S. Zhai, A. Majumdar, S. Fan and Y. Cui, *Adv. Sci.*, 2017, **3**, e1700895.
- 17 K. Lin, S. Chen, Y. Zeng, T. C. Ho, Y. Zhu, X. Wang, F. Liu, B. Huang, C. Y. H. Chao, Z. Wang and C. Y. Tso, *Science*, 2023, **382**, 691–697.
- 18 X. Zhao, T. Li, H. Xie, H. Liu, L. Wang, Y. Qu, S. C. Li, S. Liu, A. H. Brozena, Z. Yu, J. Srebric and L. Hu, *Science*, 2023, **382**, 684–691.
- 19 K. Tang, K. Dong, J. Li, M. P. Gordon, F. G. Reichertz, H. Kim, Y. Rho, Q. Wang, C. Y. Lin, C. P. Grigoropoulos, A. Javey, J. J. Urban, J. Yao, R. Levinson and J. Wu, *Science*, 2021, **374**, 1504–1509.
- 20 S. Wang, T. Jiang, Y. Meng, R. Yang, G. Tan and Y. Long, *Science*, 2021, **374**, 1501–1504.
- 21 T. Li, Y. Zhai, S. He, W. Gan, Z. Wei, M. Heidarinejad, D. Dalgo, R. Mi, X. Zhao, J. Song, J. Dai, C. Chen, A. Aili, A. Vellore, A. Martini, R. Yang, J. Srebric, X. Yin and L. Hu, *Science*, 2019, **364**, 760–763.
- 22 J. Mandal, Y. Fu, A. C. Overvig, M. Jia, K. Sun, N. N. Shi, H. Zhou, X. Xiao, N. Yu and Y. Yang, *Science*, 2018, **362**, 315–319.
- 23 Y. Zhai, Y. Ma, S. N. David, D. Zhao, R. Lou, G. Tan, R. Yang and X. Yin, *Science*, 2017, **355**, 1062–1066.
- 24 B. Zhu, W. Li, Q. Zhang, D. Li, X. Liu, Y. Wang, N. Xu, Z. Wu, J. Li, X. Li, P. B. Catrysse, W. Xu, S. Fan and J. Zhu, *Nat. Nanotechnol.*, 2021, **16**, 1342–1348.
- 25 D. Li, X. Liu, W. Li, Z. Lin, B. Zhu, Z. Li, J. Li, B. Li and S. Fan, *Nat. Nanotechnol.*, 2021, **16**, 153–158.
- 26 Z. Chen, L. Zhu, A. Raman and S. Fan, *Nat. Commun.*, 2016, **7**, 13729.
- 27 A. P. Raman, M. A. Anoma, L. Zhu, E. Rephaeli and S. Fan, *Nature*, 2014, **515**, 540–544.
- 28 X. Li, B. Sun, C. Sui, A. Nandi, H. Fang, Y. Peng, G. Tan and P. C. Hsu, *Nat. Commun.*, 2020, **11**, 6101.
- 29 E. Rephaeli, A. Raman and S. Fan, *Nano Lett.*, 2013, **13**, 1457–1461.
- 30 J. Zhou, T. G. Chen, Y. Tsurimaki, A. Hajji-Ahmad, L. Fan, Y. Peng, R. Xu, Y. Wu, S. Assaworrorarit, S. Fan, M. R. Cutkosky and Y. Cui, *Joule*, 2023, **7**, 2830–2844.
- 31 J. Li, K. Dong, T. Zhang, D. Tseng, C. Fang, R. Guo, J. Li, Y. Xu, C. Dun, J. J. Urban, T. Hong, C. P. Grigoropoulos, A. Javey, J. Yao and J. Wu, *Joule*, 2023, **7**, 2552–2567.
- 32 L. Cai, Y. Peng, J. Xu, C. Zhou, C. Zhou, P. Wu, D. Lin, S. Fan and Y. Cui, *Joule*, 2019, **3**, 1478–1486.
- 33 J. Liu, H. Tang, C. Jiang, S. Wu, L. Ye, D. Zhao and Z. Zhou, *Adv. Funct. Mater.*, 2022, **32**, 2206962.
- 34 J. Liu, J. Zhang, H. Tang, Z. Zhou, D. Zhang, L. Ye and D. Zhao, *Nano Energy*, 2021, **81**, 105611.
- 35 J. Liu, J. Zhang, D. Zhang, S. Jiao, J. Xing, H. Tang, Y. Zhang, S. Li, Z. Zhou and J. Zuo, *Renew. Sustain. Energy Rev.*, 2020, **130**, 109935.
- 36 Q. Cheng, S. Gomez, G. Hu, A. Abaalkhail, J. E. Beasley, P. Zhang, Y. Xu, X. Chen, S. Tian, J. Mandal, A. P. Raman, N. Yu, Y. Yang, Q. Cheng, S. Gomez, G. Hu, A. Abaalkhail, J. E. Beasley, P. Zhang, Y. Xu, X. Chen, S. Tian, J. Mandal, A. P. Raman, N. Yu and Y. Yang, *Nexus*, 2024, 100028.
- 37 C. Wang, H. Zou, D. Huang, R. Yang and R. Wang, *Nexus*, 2024, **1**, 100002.
- 38 D. Zhao, A. Aili, Y. Zhai, J. Lu, D. Kidd, G. Tan, X. Yin and R. Yang, *Joule*, 2019, **3**, 111–123.
- 39 A. Aili, D. Zhao, J. Lu, Y. Zhai, X. Yin, G. Tan and R. Yang, *Energy Convers. Manag.*, 2019, **186**, 586–596.
- 40 J. Liu, Y. Zhang, S. Li, C. Valenzuela, S. Shi, C. Jiang, S. Wu, L. Ye, L. Wang and Z. Zhou, *Chem. Eng. J.*, 2023, **453**, 139739.
- 41 J. Liu, J. Zhang, D. Zhang, S. Jiao, Z. Zhou, H. Tang, J. Zuo and Z. Zhang, *Sol. Energy Mater. Sol. Cells*, 2021, **220**, 110826.
- 42 J. Liu, Y. Zhang, D. Zhang, S. Jiao, Z. Zhang and Z. Zhou, *Energy Convers. Manag.*, 2020, **216**, 112923.

- 43 S. Y. Jeong, C. Y. Tso, J. Ha, Y. M. Wong, C. Y. H. Chao, B. Huang and H. Qiu, *Renew. Energy*, 2020, **146**, 44–55.
- 44 H. Fang, D. Zhao, J. Yuan, A. Aili, X. Yin, R. Yang and G. Tan, *Appl. Energy*, 2019, **248**, 589–599.
- 45 J. Liu, H. Tang, J. Zhang, D. Zhang, S. Jiao and Z. Zhou, *Energy Built Environ.*, 2023, **4**, 131–139.
- 46 J. Liu, D. Zhang, S. Jiao, Z. Zhou, Z. Zhang and F. Gao, *Sol. Energy Mater. Sol. Cells*, 2020, **207**, 110368.
- 47 J. Liu, D. Zhang, S. Jiao, Z. Zhou, Z. Zhang and F. Gao, *Sol. Energy Mater. Sol. Cells*, 2020, **208**, 110412.
- 48 J. Chen, L. Lu, Q. Gong, W. Y. Lau and K. H. Cheung, *Energy Convers. Manag.*, 2021, **245**, 114621.
- 49 Y. Gao, D. Shi, R. Levinson, R. Guo, C. Lin and J. Ge, *Energy Build.*, 2017, **156**, 343–359.
- 50 J. Liu, D. Zhang, S. Jiao, Z. Zhou, Z. Zhang and F. Gao, *Sol. Energy Mater. Sol. Cells*, 2020, **208**, 110412.
- 51 D. Han, B. F. Ng and M. P. Wan, *Sol. Energy Mater. Sol. Cells*, 2020, **206**, 110270.
- 52 B. Bhatia, A. Leroy, Y. Shen, L. Zhao, M. Gianello, D. Li, T. Gu, J. Hu, M. Soljačić and E. N. Wang, *Nat. Commun.*, 2018, **9**, 1–8.
- 53 W. Gao, Z. Lei, K. Wu and Y. Chen, *Adv. Funct. Mater.*, 2021, **31**, 2100535.
- 54 W. Huang, Y. Chen, Y. Luo, J. Mandal, W. Li, M. Chen, C. C. Tsai, Z. Shan, N. Yu and Y. Yang, *Adv. Funct. Mater.*, 2021, **31**, 2010334.
- 55 X. Wang, X. Liu, Z. Li, H. Zhang, Z. Yang, H. Zhou and T. Fan, *Adv. Funct. Mater.*, 2020, **30**, 1907562.
- 56 A. R. Gentle and G. B. Smith, *Adv. Sci.*, 2015, **2**, 1500119.
- 57 X. Zhang, *Science*, 2017, **355**, 1023–1024.
- 58 Q. Tian, X. Tu, L. Yang, H. Liu, Y. Zhou, Y. Xing, Z. Chen, S. Fan, J. Evans and S. He, *Small*, 2022, **18**, 2205091.
- 59 K. Zhang, C. Mo, X. Tang and X. Lei, *ACS Sustain. Chem. Eng.*, 2023, **11**, 7745–7754.
- 60 H. Zhong, Y. Li, P. Zhang, S. Gao, B. Liu, Y. Wang, T. Meng, Y. Zhou, H. Hou, C. Xue, Y. Zhao and Z. Wang, *ACS Nano*, 2021, **15**, 10076–10083.
- 61 T. Wang, Y. Wu, L. Shi, X. Hu, M. Chen and L. Wu, *Nat. Commun.*, 2021, **12**, 365.
- 62 J. Li, Y. Liang, W. Li, N. Xu, B. Zhu, Z. Wu, X. Wang, S. Fan, M. Wang and J. Zhu, *Sci. Adv.*, 2022, **8**, eabj9756.
- 63 Y. Du, Y. Chen, X. Yang, J. Liu, Y. Liang, Y. Chao, J. Yuan, H. Liu, Z. Zhou and J. Yan, *J. Mater. Chem. A*, 2024, **12**, 21490–21514.
- 64 Z. Cheng, H. Han, F. Wang, Y. Yan, X. Shi, H. Liang, X. Zhang and Y. Shuai, *Nano Energy*, 2021, **89**, 106377.
- 65 F. Du, W. Zhu, R. Yang, Y. Zhang, J. Wang, W. Li, W. Zuo, L. Zhang, L. Chen, W. She and T. Li, *Adv. Sci.*, 2023, **10**, 2300340.
- 66 L. Zhou, J. Rada, H. Zhang, H. Song, S. Mirniaharikandi, B. S. Ooi and Q. Gan, *Adv. Sci.*, 2021, **8**, 2102502.
- 67 M. Qin, H. Han, F. Xiong, Z. Shen, Y. Jin, S. Han, A. Usman, J. Zhou and R. Zou, *Adv. Funct. Mater.*, 2023, **33**, 2304073.
- 68 J. Wang, D. Yuan, P. Hu, Y. Wang, J. Wang and Q. Li, *Adv. Funct. Mater.*, 2023, **33**, 2300441.
- 69 X. Liu, M. Zhang, Y. Hou, Y. Pan, C. Liu and C. Shen, *Adv. Funct. Mater.*, 2022, **32**, 2207414.
- 70 T. Li, H. Sun, M. Yang, C. Zhang, S. Lv, B. Li, L. Chen and D. Sun, *Chem. Eng. J.*, 2023, **452**, 139518.
- 71 X. Zhang, X. Cheng, Y. Si, J. Yu and B. Ding, *Chem. Eng. J.*, 2022, **433**, 133628.
- 72 B. Ma, B. Wu, P. Hu, L. Liu and J. Wang, *J. Mater. Chem. A*, 2023, **11**, 15227–15236.
- 73 L. An, D. Petit, M. Di Luigi, A. Sheng, Y. Huang, Y. Hu, Z. Li and S. Ren, *ACS Appl. Nano Mater.*, 2021, **4**, 6357–6363.
- 74 C. Cai, Z. Wei, C. Ding, B. Sun, W. Chen, C. Gerhard, E. Nimerovsky, Y. Fu and K. Zhang, *Nano Lett.*, 2022, **22**, 4106–4114.
- 75 C. Ziming, W. Fuqiang, G. Dayang, L. Huaxu and S. Yong, *Sol. Energy Mater. Sol. Cells*, 2020, **213**, 110563.
- 76 X. Yu, F. Yao, W. Huang, D. Xu and C. Chen, *Renew. Energy*, 2022, **194**, 129–136.
- 77 H. Tang, S. Li, Y. Zhang, Y. Na, C. Sun, D. Zhao, J. Liu and Z. Zhou, *J. Clean. Prod.*, 2022, **380**, 135035.
- 78 S. Atiganyanun, J. B. Plumley, S. J. Han, K. Hsu, J. Cytrynbaum, T. L. Peng, S. M. Han and S. E. Han, *ACS Photonics*, 2018, **5**, 1181–1187.
- 79 X. Li, J. Peoples, P. Yao and X. Ruan, *ACS Appl. Mater. Interfaces*, 2021, **13**, 21733–21739.
- 80 X. Li, J. Peoples, Z. Huang, Z. Zhao, J. Qiu and X. Ruan, *Cell Rep. Phys. Sci.*, 2020, **1**, 100221.
- 81 J. Mandal, Y. Yang, N. Yu and A. P. Raman, *Joule*, 2020, **4**, 1350–1356.
- 82 Z. Tong, J. Peoples, X. Li, X. Yang, H. Bao and X. Ruan, *Mater. Today Phys.*, 2022, **24**, 100658.
- 83 A. Felicelli, I. Katsamba, F. Barrios, Y. Zhang, Z. Guo, J. Peoples, G. Chiu and X. Ruan, *Cell Rep. Phys. Sci.*, 2022, **3**, 101058.
- 84 J. Huang, M. Li and D. Fan, *Appl. Mater. Today*, 2021, **25**, 101209.
- 85 X. Xue, M. Qiu, Y. Li, Q. M. Zhang, S. Li, Z. Yang, C. Feng, W. Zhang, J. G. Dai, D. Lei, W. Jin, L. Xu, T. Zhang, J. Qin, H. Wang and S. Fan, *Adv. Mater.*, 2020, **32**, 1906751.
- 86 X. Nie, Y. Yoo, H. Hewakuruppu, J. Sullivan, A. Krishna and J. Lee, *Sci. Rep.*, 2020, **10**, 6661.
- 87 X. Yu, H. F. R. Chan, C. Xiao and C. Chen, *Energy Build.*, 2023, **298**, 113578.
- 88 Y. Sun, H. He, X. Huang and Z. Guo, *ACS Appl. Mater. Interfaces*, 2023, **15**, 4799–4813.
- 89 C. Park, C. Park, S. Park, J. Lee, Y. S. Kim and Y. Yoo, *Chem. Eng. J.*, 2023, **459**, 141652.
- 90 J. Peoples, Y. W. Hung, Z. Fang, J. Braun, W. T. Horton and X. Ruan, *Int. J. Heat Mass Tran.*, 2022, **194**, 123001.
- 91 S. Son, S. Jeon, D. Chae, S. Y. Lee, Y. Liu, H. Lim, S. J. Oh and H. Lee, *Nano Energy*, 2021, **79**, 105461.
- 92 X. Wang, Q. Zhang, S. Wang, C. Jin, B. Zhu, Y. Su, X. Dong, J. Liang, Z. Lu, L. Zhou, W. Li, S. Zhu and J. Zhu, *Sci. Bull.*, 2022, **67**, 1874–1881.
- 93 S. Son, S. Jeon, J. H. Bae, S. Y. Lee, D. Chae, J. Y. Chae, T. Paik, H. Lee and S. J. Oh, *Mater. Today Phys.*, 2021, **21**, 100496.
- 94 T. Y. Yoon, S. Son, S. Min, D. Chae, H. Y. Woo, J. Y. Chae, H. Lim, J. Shin, T. Paik and H. Lee, *Mater. Today Phys.*, 2021, **21**, 100510.

- 95 T. Huang, Q. Chen, J. Huang, Y. Lu, H. Xu, M. Zhao, Y. Xu and W. Song, *ACS Appl. Mater. Interfaces*, 2023, **15**, 16277–16287.
- 96 C. Sheng, Y. An, J. Du and X. Li, *ACS Photonics*, 2019, **6**, 2545–2552.
- 97 G. J. Lee, Y. J. Kim, H. M. Kim, Y. J. Yoo and Y. M. Song, *Adv. Opt. Mater.*, 2018, **6**, 1800707.
- 98 S. Yu, Q. Zhang, Y. Wang, Y. Lv and R. Ma, *Nano Lett.*, 2022, **22**, 4925–4932.
- 99 J.-W. Cho, E.-J. Lee and S.-K. Kim, *Nano Lett.*, 2022, **22**, 380–388.
- 100 J. Zhao, F. Nan, L. Zhou, H. Huang, G. Zhou, Y. fu Zhu and Q. Ou, *Sol. Energy Mater. Sol. Cells*, 2023, **251**, 112136.
- 101 J. W. Zhang, B. C. Pan, L. Xu, T. Zuo, S. Xu, T. Q. Xu, S. J. Zhong, X. Q. Yang, Y. Cai and L. M. Yi, *Adv. Eng. Mater.*, 2023, **25**, 2300062.
- 102 R. A. Yalçın, E. Blandre, K. Joulain and J. Dré villon, *ACS Photonics*, 2020, **7**, 1312–1322.
- 103 M. Chen, D. Pang and H. Yan, *Appl. Therm. Eng.*, 2022, **216**, 119125.
- 104 H. Zhai, D. Fan and Q. Li, *Sol. Energy Mater. Sol. Cells*, 2022, **245**, 111853.
- 105 W. Zhu, B. Droguet, Q. Shen, Y. Zhang, T. G. Parton, X. Shan, R. M. Parker, M. F. L. De Volder, T. Deng, S. Vignolini and T. Li, *Adv. Sci.*, 2022, **9**, 2202061.
- 106 S. Min, S. Jeon, K. Yun and J. Shin, *ACS Photonics*, 2022, **9**, 1196–1205.
- 107 X. Ma, Y. Fu, A. Portniagin, N. Yang, D. Liu, A. L. Rogach, J. G. Dai and D. Lei, *J. Mater. Chem. A*, 2022, **10**, 19635–19640.
- 108 J. Liu, Y. Liu, J. Wang, H. Li, K. Zhou, R. Gui, K. Xian, Q. Qi, X. Yang, Y. Chen, W. Zhao, H. Yin, K. Zhao, Z. Zhou and L. Ye, *Adv. Energy Mater.*, 2022, **12**, 2201975.
- 109 J. Liu, Z. Zhou, Y. Gao, Y. Wu, J. Wang, H. Li, Q. Wang, K. Zhou, K. Xian, Y. Chen, W. Zhao, F. Zhang, H. Yin, Y. Liu, K. Zhao, J. Yan and L. Ye, *Energy Environ. Sci.*, 2023, **16**, 4474–4485.
- 110 J. Liu, K. Xian, L. Ye and Z. Zhou, *Adv. Mater.*, 2021, **33**, 2008115.
- 111 J. Yuan, A. Hazarika, Q. Zhao, X. Ling, T. Moot, W. Ma and J. M. Luther, *Joule*, 2020, **4**, 1160–1185.
- 112 A. Swarnkar, A. R. Marshall, E. M. Sanehira, B. D. Chernomordik, D. T. Moore, J. A. Christians, J. M. Luther and T. Chakrabarti, *Science*, 2016, **354**, 92–96.
- 113 J. Liu, J. Qiao, K. Zhou, J. Wang, R. Gui, K. Xian, M. Gao, H. Yin, X. Hao, Z. Zhou and L. Ye, *Small*, 2022, **18**, 2201387.
- 114 R. Dong, T. Du, S. Dong, X. Zhao, R. Ma, A. Du, Y. Fan and X. Cao, *Sol. Energy Mater. Sol. Cells*, 2022, **235**, 111486.
- 115 S. Tao, X. Xu, M. Chen, W. Xu, L. Li, Z. Fang, C. Zhu, C. Lu and Z. Xu, *Sol. Energy Mater. Sol. Cells*, 2021, **224**, 110998.
- 116 Y. Gao, X. Song, A. S. Farooq and P. Zhang, *Sol. Energy*, 2021, **228**, 474–485.
- 117 J. Song, W. Zhang, Z. Sun, M. Pan, F. Tian, X. Li, M. Ye and X. Deng, *Nat. Commun.*, 2022, **13**, 4805.
- 118 C. Cai, F. Chen, Z. Wei, C. Ding, Y. Chen and Y. Wang, *Chem. Eng. J.*, 2023, **476**, 146668.
- 119 P. Yao, Z. Chen, T. Liu, X. Liao, Z. Yang, J. Li, Y. Jiang, N. Xu, W. Li, B. Zhu and J. Zhu, *Adv. Mater.*, 2022, **34**, 2208236.
- 120 H. D. Wang, C. H. Xue, X. J. Guo, B. Y. Liu, Z. Y. Ji, M. C. Huang and S. T. Jia, *Appl. Mater. Today*, 2021, **24**, 101100.
- 121 H. Luo, M. Yang, J. Guo, W. Zou, J. Xu and N. Zhao, *ACS Appl. Polym. Mater.*, 2022, **4**, 5746–5755.
- 122 S. Feng, L. Yao, M. Feng, H. Cai, X. He, X. Bu, Y. Huang, Y. Zhou and M. He, *Chem. Eng. J.*, 2023, **475**, 146191.
- 123 J. Fei, D. Han, J. Ge, X. Wang, S. W. Koh, S. Gao, Z. Sun, M. P. Wan, B. F. Ng, L. Cai and H. Li, *Adv. Funct. Mater.*, 2022, **32**, 2203582.
- 124 M. Shi, Z. Song, J. Ni, X. Du, Y. Cao, Y. Yang, W. Wang and J. Wang, *ACS Nano*, 2023, **17**, 2029–2038.
- 125 J. H. Wang, C. H. Xue, B. Y. Liu, X. J. Guo, L. C. Hu, H. Di Wang and F. Q. Deng, *ACS Omega*, 2022, **7**, 15247–15257.
- 126 X. Li, S. Shao, M. Huang, S. Zhang and W. Guo, *iScience*, 2023, **26**, 105894.
- 127 W. Yang, P. Xiao, S. Li, F. Deng, F. Ni, C. Zhang, J. Gu, J. Yang, S. W. Kuo, F. Geng and T. Chen, *Small*, 2023, **19**, 2302509.
- 128 H. Yuan, R. Liu, S. Cheng, W. Li, M. Ma, K. Huang, J. Li, Y. Cheng, K. Wang, Y. Yang, F. Liang, C. Tu, X. Wang, Y. Qi and Z. Liu, *Adv. Mater.*, 2023, **35**, 2209897.
- 129 Z. Yang, Y. Jia and J. Zhang, *ACS Appl. Mater. Interfaces*, 2022, **14**, 24755–24765.
- 130 S. Shi, P. Lv, C. Valenzuela, B. Li, Y. Liu, L. Wang and W. Feng, *Small*, 2023, **19**, 2301957.
- 131 J. Mandal, M. Jia, A. Overvig, Y. Fu, E. Che, N. Yu and Y. Yang, *Joule*, 2019, **3**, 3088–3099.
- 132 H. Zhao, Q. Sun, J. Zhou, X. Deng and J. Cui, *Adv. Mater.*, 2020, **32**, 2000870.
- 133 X. Zhao, A. Aili, D. Zhao, D. Xu, X. Yin and R. Yang, *Cell Rep. Phys. Sci.*, 2022, **3**, 100853.
- 134 Q. Zhang, Y. Lv, Y. Wang, S. Yu, C. Li, R. Ma and Y. Chen, *Nat. Commun.*, 2022, **13**, 4874.
- 135 Q. Zhang, Y. Wang, Y. Lv, S. Yu and R. Ma, *Proc. Natl. Acad. Sci. U. S. A.*, 2022, **119**, e2207353119.
- 136 G. Chen, K. Wang, J. Yang, J. Huang, Z. Chen, J. Zheng, J. Wang, H. Yang, S. Li, Y. Miao, W. Wang, N. Zhu, X. Jiang, Y. Chen and J. Fu, *Adv. Mater.*, 2023, **35**, 2211716.
- 137 Y. Deng, Y. Yang, Y. Xiao, H. Lou Xie, R. Lan, L. Zhang and H. Yang, *Adv. Funct. Mater.*, 2023, **33**, 2301319.
- 138 G. Xu, H. Xia, P. Chen, W. She, H. Zhang, J. Ma, Q. Ruan, W. Zhang and Z. M. Sun, *Adv. Funct. Mater.*, 2022, **32**, 2109597.
- 139 L. Long, S. Taylor and L. Wang, *ACS Photonics*, 2020, **7**, 2219–2227.
- 140 J. Gu, H. Wei, F. Ren, H. Guan, S. Liang, C. Geng, L. Li, J. Zhao, S. Dou and Y. Li, *ACS Appl. Mater. Interfaces*, 2022, **14**, 2683–2690.
- 141 X. Xu, J. Gu, H. Zhao, X. Zhang, S. Dou, Y. Li, J. Zhao, Y. Zhan and X. Li, *ACS Appl. Mater. Interfaces*, 2022, **14**, 14313–14320.
- 142 X. Ao, B. Li, B. Zhao, M. Hu, H. Ren, H. Yang, J. Liu, J. Cao, J. Feng, Y. Yang, Z. Qi, L. Li, C. Zou and G. Pei, *Proc. Natl. Acad. Sci. U. S. A.*, 2022, **119**, e2120557119.



- 143 M. Liu, X. Li, L. Li, L. Li, S. Zhao, K. Lu, K. Chen, J. Zhu, T. Zhou, C. Hu, Z. Lin, C. Xu, B. Zhao, G. Zhang, G. Pei and C. Zou, *ACS Nano*, 2023, **17**, 9501–9509.
- 144 K. Tang, K. Dong, J. Li, M. P. Gordon, F. G. Reichertz, H. Kim, Y. Rho, Q. Wang, C. Y. Lin, C. P. Grigoropoulos, A. Javey, J. J. Urban, J. Yao, R. Levinson and J. Wu, *Science*, 2021, **374**, 1504–1509.
- 145 S. Sheng, J. Wang, B. Zhao, Z. He, X. Feng, Q. Shang, C. Chen, G. Pei, J. Zhou, J. Liu and S. Yu, *Nat. Commun.*, 2023, **14**, 3231.
- 146 S. M. A. Durrani, E. E. Khawaja, A. M. Al-Shukri and M. F. Al-Kuhaili, *Energy Build.*, 2004, **36**, 891–898.
- 147 Z. Fang, L. Ding, L. Li, K. Shuai, B. Cao, Y. Zhong, Z. Meng and Z. Xia, *ACS Photonics*, 2021, **8**, 2781–2790.
- 148 S. Wang, Y. Dong, Y. Li, K. Ryu, Z. Dong, J. Chen, Z. Dai, Y. Ke, J. Yin and Y. Long, *Mater. Horiz.*, 2023, **10**, 4243–4250.
- 149 X. Mei, T. Wang, M. Chen and L. Wu, *J. Mater. Chem. A*, 2022, **10**, 11092–11100.
- 150 R. Zhang, R. Li, P. Xu, W. Zhong, Y. Zhang and Z. Luo, *Chem. Eng. J.*, 2023, **471**, 144527.
- 151 J. Chen, L. Lu and Q. Gong, *Appl. Energy*, 2023, **349**, 121679.
- 152 F. Bu, D. Yan, G. Tan, H. Sun and J. An, *Appl. Energy*, 2022, **312**, 118733.
- 153 D. Tian, J. Zhang and Z. Gao, *Energy Build.*, 2023, **291**, 113131.
- 154 Y. Zhang, Z. Yang, Z. Zhang, Y. Cai, Z. Sun, H. Zhang, Y. Li, L. Liu, W. Zhang, X. Xue and L. Xu, *Energy Build.*, 2023, **284**, 112702.
- 155 Y. Cai, Z. Zhang, Z. Yang, Z. Fang, S. Chen, X. Zhang, W. Li, Y. Zhang, H. Zhang, Z. Sun, Y. Zhang, Y. Li, L. Liu, W. Zhang and X. Xue, *Heliyon*, 2023, **9**, e14599.
- 156 J. Yuan, H. Yin, D. Yuan, Y. Yang and S. Xu, *Energy*, 2022, **242**, 122779.
- 157 Y. Cai, Z. Yang, Z. Zhang, Z. Yang, H. Zhang, X. Xue, M. Xian, Y. Shu, X. Gong, X. Cai, H. Jiang, Y. Li, L. Liu and W. Zhang, *Sol. Energy*, 2023, **256**, 127–139.
- 158 Y. Lei, X. Huang, X. Li and C. Feng, *Energy Build.*, 2023, **279**, 112716.
- 159 S. Chen, K. Lin, A. Pan, T. C. Ho, Y. Zhu and C. Y. Tso, *Renew. Energy*, 2023, **211**, 326–335.
- 160 K. Zhang, D. Zhao, X. Yin, R. Yang and G. Tan, *Appl. Energy*, 2018, **224**, 371–381.
- 161 F. Bu, D. Yan, G. Tan, H. Sun and J. An, *Renew. Energy*, 2023, **202**, 255–269.
- 162 D. Shen, C. Yu and W. Wang, *Appl. Therm. Eng.*, 2020, **176**, 115479.
- 163 S. Tao, Q. Wan, Y. Xu, D. Gao, Z. Fang, Y. Ni, L. Fang, C. Lu and Z. Xu, *Energy Build.*, 2023, **288**, 113031.
- 164 M. Gálvez, J. García, R. Barraza and J. Contreras, *Energy Build.*, 2021, **252**, 111364.
- 165 C. Yu, D. Shen, W. He, Z. Hu, S. Zhang and W. Chu, *Renew. Energy*, 2021, **178**, 1057–1069.
- 166 Z. Chen, L. Zhu, W. Li and S. Fan, *Joule*, 2019, **3**, 101–110.
- 167 L. Zhou, H. Song, N. Zhang, J. Rada, M. Singer, H. Zhang, B. S. Ooi, Z. Yu and Q. Gan, *Cell Rep. Phys. Sci.*, 2021, **2**, 100338.
- 168 J. Peoples, Y. W. Hung, X. Li, D. Gallagher, N. Fruehe, M. Pottschmidt, C. Breseman, C. Adams, A. Yuksel, J. Braun, W. T. Horton and X. Ruan, *Appl. Energy*, 2022, **310**, 118368.
- 169 L. Zhou, H. Song, J. Liang, M. Singer, M. Zhou, E. Stegenburgs, N. Zhang, C. Xu, T. Ng, Z. Yu, B. Ooi and Q. Gan, *Nat. Sustain.*, 2019, **2**, 718–724.
- 170 J. Liu, H. Tang, D. Zhang, S. Jiao, Z. Zhou, Z. Zhang, J. Ling and J. Zuo, *Energy*, 2020, **211**, 118618.
- 171 J. Liu, Z. Zhou, D. Zhang, S. Jiao, Y. Zhang, L. Luo, Z. Zhang and F. Gao, *Renew. Energy*, 2020, **155**, 90–99.
- 172 S. Li, Z. Zhou, J. Liu, J. Zhang, H. Tang, Z. Zhang, Y. Na and C. Jiang, *Renew. Energy*, 2022, **198**, 947–959.
- 173 H. Tang, Z. Zhou, S. Jiao, Y. Zhang, S. Li, D. Zhang, J. Zhang, J. Liu and D. Zhao, *Sol. Energy Mater. Sol. Cells*, 2022, **235**, 111498.
- 174 D. Zhao, A. Aili, X. Yin, G. Tan and R. Yang, *Energy Build.*, 2019, **203**, 109453.
- 175 D. Xu, S. Boncoeur, G. Tan, J. Xu, H. Qian and D. Zhao, *Build. Simulat.*, 2022, **15**, 167–178.
- 176 D. Zhao, X. Yin, J. Xu, G. Tan and R. Yang, *Energy*, 2020, **190**, 116322.
- 177 M. Hu, G. Pei, Q. Wang, J. Li, Y. Wang and J. Ji, *Appl. Energy*, 2016, **179**, 899–908.
- 178 M. Hu, B. Zhao, X. Ao, N. Chen, J. Cao, Q. Wang, Y. Su and G. Pei, *Sol. Energy*, 2020, **197**, 332–343.
- 179 M. Hu, B. Zhao, X. Ao, Y. Su and G. Pei, *Energy*, 2018, **165**, 811–824.
- 180 M. Hu, B. Zhao, S. Suhendri, J. Cao, Q. Wang, S. Riffat, R. Yang, Y. Su and G. Pei, *Appl. Energy*, 2022, **306**, 118096.
- 181 B. Zhao, M. Hu, X. Ao, N. Chen, Q. Xuan, Y. Su and G. Pei, *Energy*, 2019, **183**, 892–900.
- 182 B. Zhao, J. Liu, M. Hu, X. Ao, L. Li, Q. Xuan and G. Pei, *Renew. Energy*, 2023, **205**, 763–771.
- 183 S. Suhendri, M. Hu, Y. Su, J. Darkwa and S. Riffat, *Build. Environ.*, 2022, **225**, 109648.
- 184 A. P. Raman, W. Li and S. Fan, *Joule*, 2019, **3**, 2679–2686.
- 185 K. Te Lin, J. Han, K. Li, C. Guo, H. Lin and B. Jia, *Nano Energy*, 2021, **80**, 105517.
- 186 X. Yu, J. Chan and C. Chen, *Nano Energy*, 2021, **88**, 106259.
- 187 S. Fan and W. Li, *Nat. Photonics*, 2022, **16**, 182–190.
- 188 B. Xie, Y. Liu, W. Xi and R. Hu, *Mater. Today Energy*, 2023, **34**, 101302.
- 189 J. Xue, J. W. Lee, Z. Dai, R. Wang, S. Nuryyeva, M. E. Liao, S. Y. Chang, L. Meng, D. Meng, P. Sun, O. Lin, M. S. Goorsky and Y. Yang, *Joule*, 2018, **2**, 1866–1878.
- 190 J. Yuan, X. Ling, D. Yang, F. Li, S. Zhou, J. Shi, Y. Qian, J. Hu, Y. Sun, Y. Yang, X. Gao, S. Duhm, Q. Zhang and W. Ma, *Joule*, 2018, **2**, 2450–2463.
- 191 E. M. Sanehira, A. R. Marshall, J. A. Christians, S. P. Harvey, P. N. Ciesielski, L. M. Wheeler, P. Schulz, L. Y. Lin, M. C. Beard and J. M. Luther, *Sci. Adv.*, 2017, **3**, eaao4204.
- 192 Y. An, Y. Fu, D. Jian-Guo, X. Yin and D. Lei, *Cell Rep. Phys. Sci.*, 2022, **3**, 101098.